Pergamon

PII: S0191-8141(97)00022-9

Journal of Structural Geology, Vol. 19, No. 7, pp. 955 to 974, 1997

0191-8141/97 $17.00 + 0.00

Formation, burial and exhumation of basement nappes at crustal scale: a geometric model based on the Western Swiss–Italian Alps

ARTHUR ESCHER

Institut de Géologie, BFSH-2, Université de Lausanne, CH-1015 Lausanne, Switzerland

and

CHRISTOPHER BEAUMONT

Oceanography Department, Dalhousie University, Nova Scotia, Halifax, Canada B3H 4J1

(*Received* 23 *May* 1996; *accepted in revised form* 31 *January* 1997)

Abstract—Information from geological and reflection seismic data from the Western Swiss–Italian Alps, and from numerical models, is used to build a geometrical model that can explain some of the major tectonic–metamorphic features of Alpine-type basement nappes. The model gives a geometrical and mechanical explanation for the initiation, burial, and subsequent uplift and partial exhumation of basement nappes at a crustal scale. Three main tectonic stages during convergence are distinguished and each correlated with the formation of specific nappe structures. The first two stages are single vergent (NW) and correspond to the subduction of continental margin crust, and the formation and uplift of high-pressure rocks. Simple-shear flow and superimposed wedge-shaped pure shear flow is proposed for the creation and intrusion of high-pressure nappes of the Monte Rosa type. The third stage is characterized by a doubly-vergent style with both pro- and retro-movements. The former created NW-vergent nappes, as seen in the external Alpine massifs and the latter caused backfolding and thrusting, typical of the internal Alps. This third stage corresponds to the Neoalpine movements in the Western Swiss–Italian Alps, and is accompanied by a generalized uplift, mountain building and molasse sedimentation. © 1997 Elsevier Science Ltd.

INTRODUCTION

The scope of this paper is to give a geometrical and mechanical explanation for the initiation and subsequent uplift and stacking of basement nappes in an Alpine-type orogen. The proposed model is based mostly on information from geological and reflection seismic data from the Western Swiss–Italian Alps and, for the last (doubly-vergent) stage, on plane-strain finite-element models (Beaumont *et al.*, 1996). It tries to explain the main tectonic–metamorphic features of basement nappes and includes a relatively new concept concerning the rapid uplift and decompression of units that underwent high-pressure metamorphism. The model only deals with some of the essential characteristics of basement nappes and their evolution, and not with the highly complex details of the Swiss–Italian Alps. Moreover, it is based on two-dimensional reconstructions along vertical transverse sections which, although they contain most of the early Tertiary Alpine strain movements, do not include important longitudinal components. For these reasons the following pages are only meant to show how some old and new concepts can be applied to the orogenic deformation of basement rocks at a crustal scale. They certainly should be confirmed by more detailed work, in the field and laboratory, as well as by finite-element and analogue modeling techniques. In order to understand better the proposed model, an outline of the structure and evolution of the Western Swiss–Italian Alps is given below.

STRUCTURE OF THE WESTERN SWISS–ITALIAN ALPS

Since the early investigations (Gerlach, 1869; Schardt, 1907; Argand, 1911, 1916; Lugeon, 1914; Heim, 1921; Hermann, 1937), the geological knowledge of the Western Swiss–Italian Alps has been steadily refined by a large number of geologists. The results of the recent deep seismic survey of the Ecors-Crop and NFP-20 programs (Frei *et al.*, 1990; Tardy *et al.*, 1990; Heitzmann *et al.*, 1991; Pfiffner, 1992; Marchant, 1993; Escher *et al.*, 1997; Steck *et al.*, 1997) have allowed us for the first time to control to some extent the geometric extrapolations and reconstructions of the deep Alpine structures. The result, although not very different to Argand's brilliant reconstruction, gives a better impression of the geometry of each Alpine unit at a crustal scale. It also shows the probable relationship between the Alpine nappe stack and the European and Adriatic lithospheres. In a simplified way, these data are represented in the geological cross-section of Fig. 1 which trends from the Mont Tendre (Jura) to the Val Sesia (Sesia-Ivrea). The site of this profile was chosen because it crosses one of the best-known parts of the Alpine chain; because many of the geological interpretations of the seismic profiles W1–W5 can be directly projected onto it (Escher *et al.*, 1987, 1993; Steck *et al.*, 1989; Marchant, 1993) and because the NW–SE orientation of the section coincides with the major stretching and flow direction during the paroxysm of Tertiary

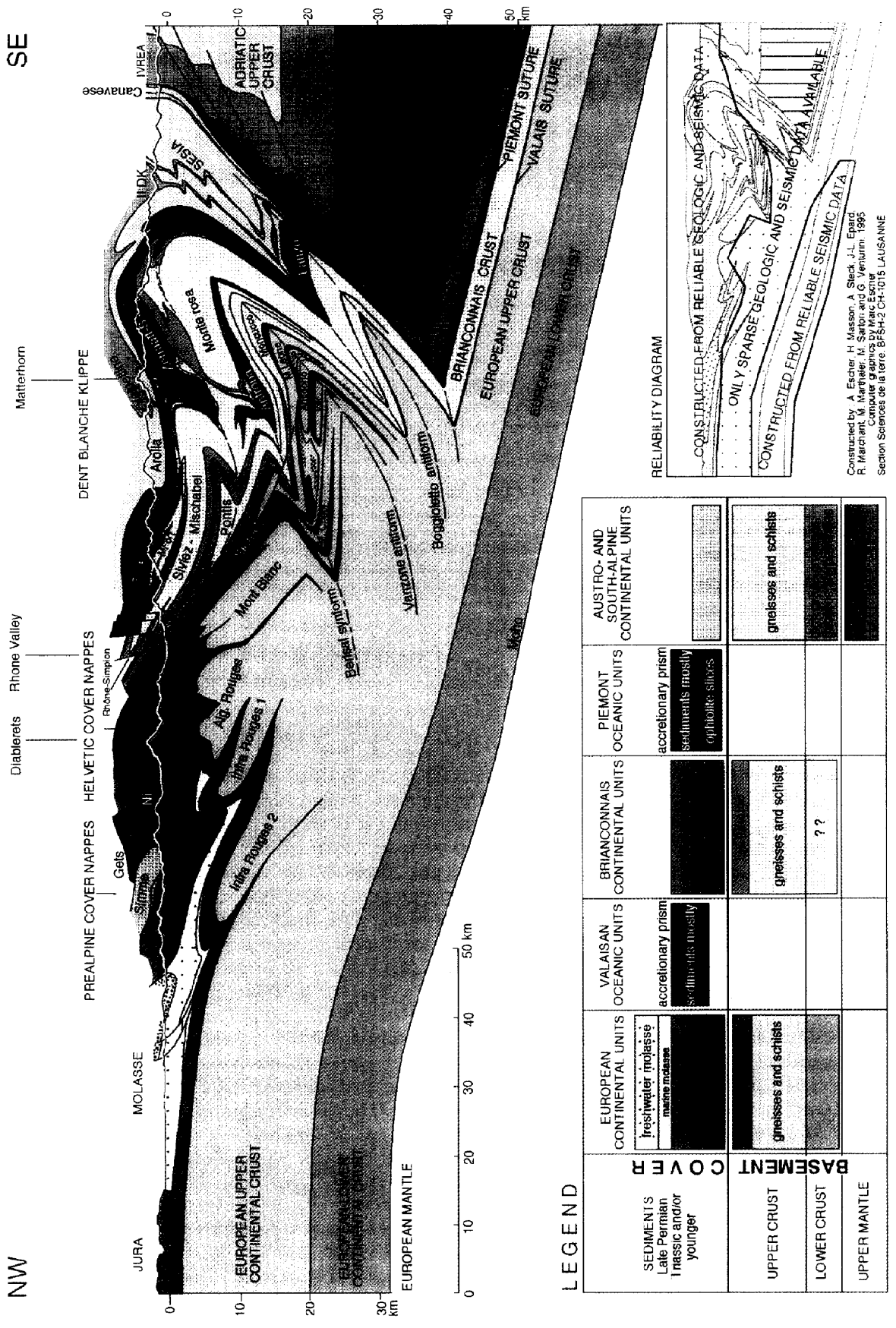

Fig. 1. Schematic geological profile through the Western Swiss–Italian Alps from the Mont Tendre (Jura) in the northwest to the Val Sesia (Sesia-Ivrea) in the southeast. It is based partly on the results of recent seismic data. The overall structure, if correctly interpreted, shows that the main response to compressional stress was the subduction of the European (and Briançonnais) lithospheres. It also demonstrates that the deformation and stacking of nappes took place within the upper part of the downgoing continental crust, while the lower crust subducted in a passive way together with the lithospheric mantle (modified after Epard and Escher, 1996 and Escher *et al.*, in press).

deformation (D_1 phase according to the classification by Steck, 1984, 1990).

As recognized by Trümpy (1973,1980,1988, 1992), Stampfli and Marthaler (1990), Stampfli (1993) and Marchant and Stampfli, 1997, the Western Swiss–Italian Alps result from the collision between at least five main lithospheric units, from the northwest or external to the southeast or internal part (Fig. 1): (1) the European continental lithosphere; (2) the Valais oceanic lithosphere; (3) the Briançonnais continental lithosphere; (4) the Piemont oceanic lithosphere; and (5) the Austroalpine and South Alpine lithospheres.

The continent-derived units are preserved as crustal basement and cover nappes, whereas only ophiolite slices and associated sediments remain of the oceanic lithospheres, forming remnants of accretionary prisms. By definition, the Alpine cover rocks were deformed by the Alpine orogeny only. Most basement rocks were also affected by earlier events. Cover rocks are mostly represented by sediments or metasediments of Late Permian–Pliocene age (Fig. 1).

Units derived from the European continental lithosphere

The European upper continental crust and cover is well represented in the external (NW) part of the belt, now forming the major component of the Swiss Alpine chain. Most structures show an initial N- to W-vergence, whereas later backfolding (S-vergence) is only observed southeast of the Aiguilles Rouges massif. The large majority of basement nappes, from the external Mont Blanc to the internal Monte Leone nappe, display fold-nappe structures. with a normal limb, a frontal hinge part and an overturned lower limb (Steck, 1984, 1987). It is likely that the most external Aiguilles Rouges and Infra Rouges basement units are also fold nappes, as inferred from seismic data (Steck *et al.*, 1997) and from outcrop features (Badoux, 1962). Alpine deformation of the basement gneisses is intense in the overturned limbs, and decreases towards the core and upper limb of each fold nappe. As a general rule, the amount of strain increases considerably from the external Aiguilles Rouges, where it is partitioned into separate shear zones, to the more internal units, where it resulted in a well-developed, penetrative and principal schistosity. This early deformation took place at greenschist-facies conditions in the external nappes, and at amphibolite facies in the more internal ones. Most internal nappes were formed during at least two successive early phases, resulting in spectacular superposed structures. Later backfolding is mostly characterized by retrograde greenschist-facies metamorphism; it always refolds earlier NW-vergent nappes.

Most of the cover of the European upper crust was detached during the formation of the basement nappes. It was displaced to the northwest, the distance of transport increasing toward the southeast. This cover is now found as external thrust sheets (Jura) or as a stack of more internal thrust and fold nappes, forming the Helvetic cover nappes (Fig. 1). Most cover thrust nappes used weak layers such as Triassic evaporites as detachment horizons. Basement and cover nappes were generated simultaneously, often by different mechanisms, ductile for the basement fold nappes and brittle for the cover thrust sheets (Escher *et al.*, 1993; Epard and Escher, 1996).

The European lower crust is well defined on most reflection seismic profiles and can be constructed down to *ca* 45 km depth (Steck *et al.*, 1997). It shows a remarkable continuity and appears to be almost undeformed by the Alpine orogen.

Units derived from the Valais oceanic lithosphere

Remnants of the Valais oceanic lithosphere and associated sediments are found in a discontinuous zone at the boundary between nappes derived from the European crust and those of Briançonnais origin (Fig. 1). The ductile oceanic sediments of the Valais accretionary prism must have formed a weak structural link between the European and Briançonnais nappe piles.

Units derived from the Briançonnais continental lithosphere

The basement nappes derived from the Briançonnais upper continental crust form a central zone between the Valais and the Piemont ophiolitic nappes (Fig. 1). Most of the Briançonnais sedimentary cover was separated from its basement during early Alpine deformations, and translated to the northwest. It forms the bulk part of the Prealpine nappes. Like the European units, the Briançonnais-derived basement nappes mostly display fold features with intensely sheared inverted limbs and less-deformed cores and upper limbs (Lacassin, 1987; Escher, 1988; Sartori, 1990). A dominant penetrative foliation, resulting from the earliest phases of deformation, is present almost everywhere. It clearly indicates that here, too, crustal nappes were formed at an early stage by heterogeneous ductile shear. Prograde greenschist-facies metamorphic conditions prevailed during the early deformation phases in the external Briançonnais nappes (Pontis, Siviez-Mischabel). In the most internal units (Mont Fort and Monte Rosa) remnants of early mineral paragenesis indicate that they were formed under high-pressure–intermediate-temperature conditions with values of *ca* 15 kbars and 500°C for parts of the Monte Rosa nappe (Bearth, 1952; Hunziker, 1970; Frey *et al.*, 1976; Colombi, 1989). Subsequently they must have been elevated, decompressed and cooled to greenschist-facies conditions before any significant heating above *ca* 500°C could take place by the terrestrial heat flow. Late SE-vergent backfolding, associated with retrograde greenschist-facies metamorphism, affected all the Briançonnais basement nappes. The Briançonnais lower crust has not been identified anywhere.

Units derived from the Piemont oceanic lithosphere

Remains of the Piemont oceanic domain form an important and continuous zone separating the Briançonnais units from the Austroalpine and Adriatic ones (Fig. 1). It is composed of two main units.

(1) The Tsate nappe is probably the remnant of an accretionary prism formed during the Early–Middle Cretaceous subduction and closure of the Piemont oceanic domain (Marthaler and Stampfli, 1989; Stampfli and Marthaler, 1990). It is mostly composed of calcschists containing lenses of ophiolitic rocks. The metamorphic history of the Tsate nappe is characterized by an early, middle–high-pressure event resulting in the formation of greenschist to blueschist metamorphic assemblages (Dal Piaz, 1976; Caby, 1981; Ayrton *et al.*, 1982; Pfeiffer *et al.*, 1989, 1991). It was followed by a pervasive greenschist-facies episode.

(2) The Zermatt-Saas and Antrona zones are large slices of Piemont oceanic lithosphere, associated with some oceanic sediments (Bearth, 1967). They underwent a very high-pressure metamorphism, probably during the Eoalpine subduction, with *P–T* conditions of *ca* 18 kbars/550°C (Hunziker, 1974; Meyer, 1983; Barnicoat and Fry, 1986; Barnicoat *et al.*, 1991). A later Tertiary greenschist (Zermatt-Saas Fee) and amphibolite facies (Antrona) overprint is well documented (Laduron, 1976; Colombi and Pfeiffer, 1986; Ganguin, 1988; Steck, 1989). In Fig. 1, the Lanzo oceanic unit is interpreted as the internal and southwest continuation of the Zermatt-Saas Fee ophiolites as proposed by Blake *et al.* (1980) and Lagabrielle *et al.* (1989).

Units derived from the Austroalpine and South Alpine continental lithospheres

South of the Piemont ophiolite suture zone, the western equivalents of the Austroalpine nappes are present in the Dent Blanche klippe and in the Sesia zone. Both are made of the same two superposed Austroalpine basement thrust nappes characterized by the absence of inverted limbs and the presence of important basal mylonites (Fig. 1).

(1) The lower nappe is composed of the Arolla series, the Gneiss Minuti and the Eclogitic Micaschist Complex (lower Sesia). It is made of (Adriatic?) upper crust and contains relic zones of high-pressure paragenesis of Cretaceous age (Venturini *et al.*, 1991; Venturini, 1995).

(2) The upper nappe comprises the Valpelline zone and the II-DK (second dioritic kinzingitic) zone, and consists of lower crust gneisses displaying well-preserved pre-Alpine granulite-facies assemblages (Argand, 1934; Dal Piaz *et al.*, 1971; Pognante *et al.*, 1988). These rocks are quite similar to those of the Ivrea (Adriatic) lower crust (Rivalenti *et al.*, 1984; Zingg *et al.*, 1990; Rutter *et al.*, 1993). High-pressure metamorphism is only present in the II-DK zone where it reaches high-grade blueschist facies.

The Vanzone and Boggioletto backfolds affect the Austroalpine nappes, as well as the underlying Piemont, Briançonnais and European crusts.

The Canavese zone, represented by a tectonically thinned zone of crustal basement and cover rocks, forms an independent unit between the exhumed Austroalpine system and the Southern Adriatic Alps. Rare serpentinized peridotite and metabasalt lenses suggest that a Canavese oceanic lithosphere has existed. The Canavese zone is limited to the northwest by an important thrust surface: the Canavese Line.

The Ivrea zone represents a unique cross-section through the Adriatic lower continental crust (Fig. 1). It is here that the Southern Alpine Moho comes closest to the present erosional surface. The lower crust is composed of granulite-facies pre-Alpine gneisses containing slices of mafic and ultramafic rocks (Schmid, 1967; Bertolani, 1968; Steck and Tièche, 1976; Zingg *et al.*, 1990). Alpine greenschist-facies metamorphism is only observed along some isolated shear zones and along the Canavese Line. The present position and the subvertical to overturned dips of the Canavese and Ivrea rocks are the result of Tertiary ductile backfolding associated with shear zones, because 'brittle' backthrusting alone could not have caused the observed orientations and dips of the gneisses.

Flysch and molasse deposits

Flysch-type sediments are, by definition, marine sediments deposited in tectonic active regions. Their age varies from Middle Cretaceous in the southeast to Late Eocene in the northwest. These flysch basins thus migrated from the southeast to the northwest, together with the advancing front of deformation (Fig. 2). During the Early Oligocene the flysch sedimentation changed into molasse type (mostly continental) in both northwest and southeast frontal basins. This coincided with the first backward movements in the southeast.

OUTLINE OF THE EVOLUTION OF THE WESTERN SWISS–ITALIAN ALPS

Following proposals of Dal Piaz *et al.* (1972), Trümpy (1973, 1980), Debelmas *et al.* (1980), Hunziker and Martinotti (1984), Hunziker *et al.* (1989, 1992), Steck and Hunziker (1994), Escher *et al.* (1997), the orogenic history of the Western Swiss–Italian Alps can be divided into three main periods of tectono-metamorphic activity (Fig. 2).

(1) The *Eoalpine* orogenic events, Cretaceous–Early Paleocene in age with a peak of metamorphic pressure reached at about 110 Ma and a temperature peak at 85 Ma. These events are characterized by the formation of high-pressure mineral assemblages.

(2) The *Mesoalpine* orogenic events, which we propose

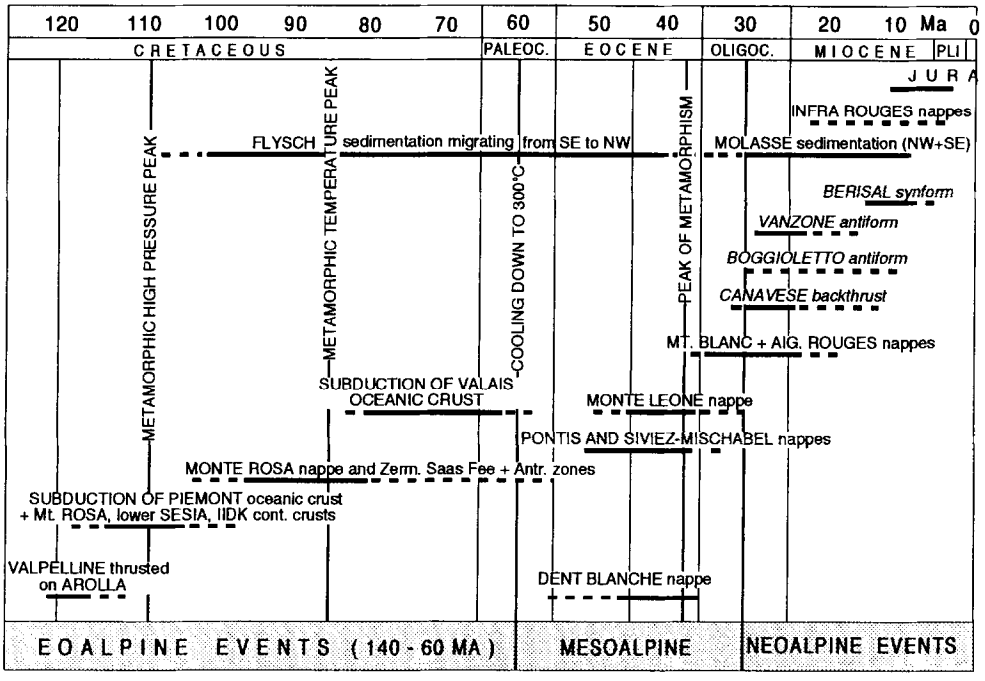

Fig. 2. Chronology of some of the major structural and metamorphic events during the Cretaceous and Tertiary in the Western Swiss–Italian Alps (mainly after Trümpy, 1980, Steck and Hunziker, 1994 and Escher *et al.*, 1997).

to extend from the Late Paleocene to the Early Oligocene, with a peak of metamorphism at around 38 Ma.

(3) The *Neoalpine* orogenic events, of Late Oligocene and younger age, characterized by the onset of backfolding, retrograde metamorphism, uplift, erosion, molasse-type sedimentation and deformation of the foreland (Jura).

The Eoalpine orogenic events (140–60 Ma)

The Eoalpine stacking of Austroalpine nappes probably took place at an early stage of subduction to the southeast of the Piemont oceanic crust. It could have resulted from a breakup of the thinned Austroalpine (= Adriatic?) marginal continental crust into imbricate slices, in parts dragged down together with the subducting oceanic crust. This would explain the high-pressure metamorphism of the lower Sesia and IIDK zones (Vuichard, 1989). The subduction of the Piemont oceanic lithosphere was probably followed by that of the thinned marginal Briançonnais continental crust, up to a depth of at least 80 km in order to permit the formation of the high-pressure metamorphic rocks. At the end of the Eoalpine events, a Late Cretaceous–Early Paleocene phase (85–60 Ma) was characterized by the uplift and decompression of the high-pressure rocks (Oberhänsli *et al.*, 1985; Hunziker *et al.*, 1989; Hurford and Hunziker, 1989). During this phase high-pressure rocks of the Zermatt-Saas Fee–Monte Rosa composite nappe came into contact with overlying intermediate- to low-pressure rocks of the Tsate nappe. This created a normal fault contact (the Combin detachment fault), the object of stimulating models of extensional movements combined with exhumation and erosion (Platt, 1986; Merle and Ballèvre, 1992).

The Mesoalpine orogenic events (60–30 Ma)

The Mesoalpine events caused the deformation of two hitherto undisturbed parts of the Alpine domain: the central part of the Briançonnais and the internal part of the European continental crust. Deformation was caused mainly by continental subduction to the southeast, in geometric continuation of the preceding Piemont and Valais oceanic subductions. Strain accumulated essentially in the upper crust by pervasive ductile shear of the basement rocks and by décollement of cover sequences. It resulted in the formation and stacking of ductile basement nappes. During this process, the Mesozoic cover was expelled towards the northwest, forming the main body of the Prealpine cover nappes (Fig. 1). It escaped thus the intense deformation and metamorphism of the basement units. At the same time the earlier formed Eoalpine nappe stack (Valpelline-Arolla) probably advanced further on top of the Briançonnais-derived units, thereby forming the Dent Blanche nappe. At the end of the Mesoalpine period, the internal European crustal units were thrust below the external Briançonnais ones, and the first Helvetic nappes began to take shape. According to Steck (1984) and Lacassin (1989), this event was accompanied by an important dextral horizontal movement of at least 40 km along the Simplon shear zone. Prograde metamorphism during the Mesoalpine deformation took place at temperatures above 300°C in

most basement rocks. A peak of metamorphism was reached around 38 Ma (Hunziker, 1974; Hunziker *et al.*, 1989). Subsequent cooling, related to updoming and erosion, is recorded by the cooling curves of the Monte Rosa and Siviez-Mischabel nappes (Steck and Hunziker, 1994).

The Neoalpine orogenic events (30–0 Ma)

The Neoalpine orogenic events started around 30 Ma ago, after a short period of magmatic activity along the Periadriatic Line. They are characterized by intensive S- and SE-vergent backfolding and thrusting together with strong dextral strike-slip movements in the more internal part of the Western Alps. Backward movements started in the southeast and migrated to the northwest, while forward folding and thrusting continued to take place in the more external zones. The onset of large-scale S- to SE-vergent movements, combined with a continuing NW-vergent ductile shearing, initiated the present wedge shape of the Western Alps as seen on vertical sections (Fig. 1). The combination of northwest and southeast movements also produced, probably for the first time, a generalized uplift, exhumation and erosion with deposition of molasse sediments along the peripheral foredeep basins. Retrograde metamorphism (mostly greenschist facies) and uplift accompanies, as a rule, the retro-movements in the Western Swiss–Italian Alps.

CONSTRAINTS USED IN THE CONSTRUCTION OF THE GEOMETRIC MODEL

In constructing an acceptable geometric–kinematic model for the evolution of the basement nappes we have been guided by some basic results from numerical models, some physical assumptions, and constraints derived directly from geological observations described earlier. The model is incomplete, provisional and makes no attempt to explain geological details. When combining some old concepts with new ones, we have extrapolated on the numerical model results. Until these extrapolations have been tested they are best regarded as conceptual ideas.

Framework from geodynamical numerical models

At the crustal scale the Alpine evolution consisted of an Eoalpine and Mesoalpine single vergence, asymmetric subduction of Piemont, Briançonnais, Valaisan and European margin elements. It was followed by a Neoalpine collisional orogenesis with double vergence, backfolding and uplift. Both main phases can be explained by a simple mechanical model (Beaumont *et al.*, 1996). In this model, lithosphere is initially flexed downward by its negative buoyancy, thereby allowing a significant volume of crustal material to be partly subducted, highly sheared and tectonically underplated beneath the overriding Adriatic plate. Later, increased buoyancy of the subducting slab and the introduction of thicker continental crust into the subduction zone reduce the proportion of the convergent material that can be accommodated by subduction without deformation. This restriction initiates the backfolding/retro-charriage. Within the model framework, the ensuing collisional phase creates a doubly-vergent orogen with pro- and retro-tectonic wedges that face outward onto the subducting (pro-) and overriding (retro-) plates (Willett *et al.*, 1993; Beaumont and Quinlan, 1994). Some of the material subducted and underplated in the first phase is transported retroward in the hanging wall of the retro-step-up shear (Beaumont *et al.*, 1996). Depending on the surface denudation and the scale of the orogen, material from depths of ~20 to 30 km may be exhumed to the surface by this mechanism. The model pro-wedge continues to develop synchronously with the retro-charriage and growth of the retro-wedge. In the broadest sense this second phase explains the coeval backfolding and development of the external basement nappes and massifs, and the strong uplift of the Alpine wedge.

Physical assumptions

The following physical assumptions were made for construction of the model.

(1) Material volumes in the two-dimensional cross-section are conserved. Material movement in or out of the section and volume changes owing to metamorphic reactions, etc. are not considered.

(2) The main direction of tectonic motion is in the plane of the section.

(3) The minimum temperature for ductile deformation in the upper continental crust is approximately 300°C (lower greenschist facies). This limit for the brittle–ductile transition in most continental crust rocks has been accepted by many authors (e.g. Handy, 1989, 1990). By ductility we mean the capacity of a material to deform by pervasive viscous flow in shear zones over 1 km wide. We follow here more or less the definitions by Rutter (1986) and Schmid and Handy (1991).

(4) Ductile deformation occurs first by simple shear on low-angle (20–30° dip) shear zones and later becomes more pervasive and is accompanied by pure shear.

(5) Flexural isostatic adjustment at the lithospheric scale occurs rapidly by comparison with tectonics. Therefore, each step in the reconstruction is assumed to be in quasi-isostatic equilibrium except where specific loads act (for example the negative buoyancy of subducted oceanic slabs).

(6) Erosion is relatively inefficient and occurs at 0.1–0.4 of the rate of tectonic–isostatic vertical velocities.

(7) Heat transfer is included conceptually assuming that thermal re-equilibration at depths between 20 and 60 km takes ~15–25 Ma.

Geological constraints

The following geological constraints are partly deduced from the data available from the Western Swiss–Italian Alps, as summarized above, and partly assumed.

(1) Most ductile deformation of crystalline basement was limited to the subducting upper continental crust in a zone situated between the 300° isotherm and the lower continental crust.

(2) Parts of the upper continental crust became detached from the down-going lithosphere when buried at depths of *ca* 70 km during Eoalpine events (high-pressure metamorphism) and at depths of 40–12 km during the later Meso- and Neoalpine deformations. This detached upper crust progressively increased the total volume of material accumulated between the overriding and subducting lithospheres and created the Alpine belt.

(3) During detachment ductile basement (crustal) nappes were formed, mostly as W- to N-vergent fold nappes (Handy *et al.*, 1993; Schmid *et al.*, 1997), by basal simple shear and superimposed pure shear. These nappes started to be generated at important depths in the southeast and the mechanism migrated progressively to lower depths and to the northwest during continuing lithospheric subduction. The final result resembles a systematic stacking of nappes from the southeast to the northwest, forming a pro-wedge.

(4) The formation of ductile basement nappes was, as a rule, accompanied by detachment of cover rocks, often forming thrust sheets, stacked in front (i.e. to the northwest) of the basement nappe pile to form a pro-ward migrating cover nappe pile (Epard and Escher, 1996).

(5) Retro-movements, like backfolding or backthrusting, toward the southeast only started during the Neoalpine events after the formation of several important crustal pro-nappes. These retro-movements migrated from the southeast to the northwest, forming a succession of large-scale backfolds. Retro-movements in the southeast and pro-movements in the northwest probably occurred simultaneously during the Neoalpine period.

(6) The formation of W- to N-vergent pro-nappes was generally accompanied by burial and prograde metamorphism. In contrast, during SE-vergent retro-deformation crustal rock displacement was mainly upwards and metamorphism mostly retrograde.

(7) During the Eoalpine and possibly Mesoalpine events, high-pressure–intermediate-temperature metamorphic rocks formed in deep basement nappes (Monte Rosa, Mont Fort). Subsequently, these rock units moved upwards before re-equilibration of the isotherms and before the onset of retro-movements.

(8) The lower continental crust (Briançonnais and European) remained attached to the subducting mantle rocks. It is directly overlain by the weakest part of the upper crust, which probably acted as a potential zone of decoupling (Handy and Zingg, 1991; Pfiffner *et al.*, 1991; Hitz and Pfiffner, 1994).

(9) The Valais and Piemont accretionary prisms played a very important role during the build up of the Alpine belt. Their high content of pore fluids and of ductile sedimentary rocks such as calc-schists, made them the ideal detachment units between the downgoing and overriding lithospheres.

(10) Syn-tectonic sedimentation was characterized by marine flysch deposits during the Eoalpine and Mesoalpine periods and by shallow marine or continental molasse sedimentation during the Neoalpine events. This implies that a generalized uplift, exhumation and erosion of the Alpine range corresponds to the onset of the Neoalpine backfolding.

SIMPLIFICATIONS AND INITIAL STAGE OF THE MODEL

Simplifications used in the model

The proposed model describes the evolution of a general Alpine-type orogen. It is mainly inspired by the Western Swiss–Italian Alps but is simplified in the following ways in order to focus on the sequence of different processes rather than on the products of repeated processes.

(1) Only one main oceanic subduction zone and corresponding accretionary prism is considered (Fig. 3). Compared to the Alps they are the equivalents of the Piemont oceanic crust and the Tsate prism.

(2) In the overriding (SE) unit the very complex Austroalpine nappe stack is only represented by three symbolical basement thrust sheets (Fig. 3). The model concerns an explanation of events post-dating this Early Cretaceous tectonic phase.

(3) During the evolution of the model only five main NW-vergent basement nappes and three zones of backfolding and thrusting are formed successively. They represent the many more pro- and retro-structures found in the Alps.

(4) The shape of each tectonic unit is highly simplified and represented with a smooth, rounded, nappe geometry. In reality each basement nappe is, of course, made of many parasitic folds and thrusts at various scales. These detail structures are considered as meaningless at the scale considered.

(5) No distinction has been made in the cover between the many thrust sheets and fold nappes which exist in the Alps. Our model is basically meant to explain the structural history of the interface separating the Mesozoic sedimentary cover from the gneissic basement.

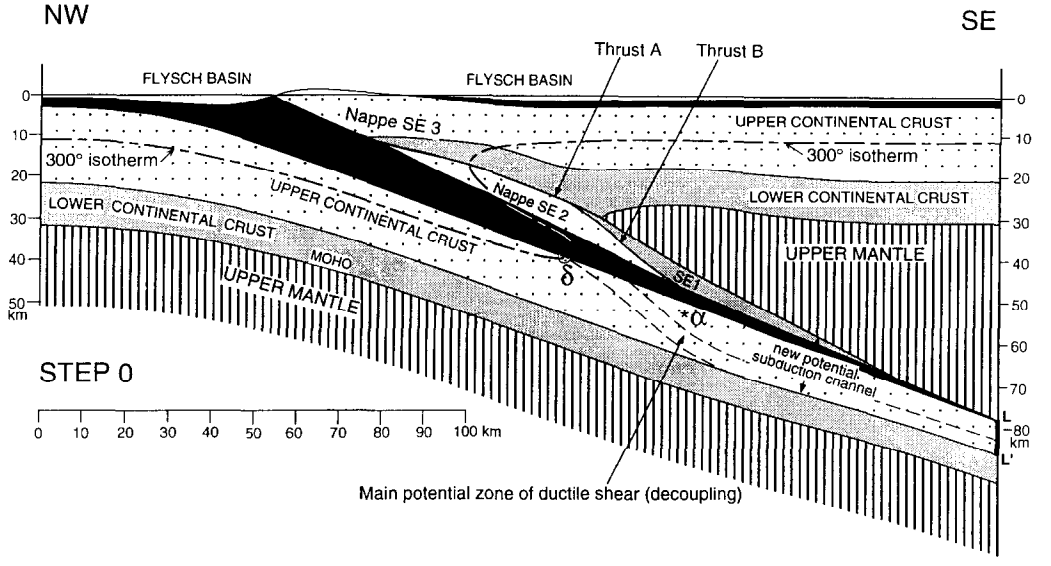

Fig. 3. (Step 0 of the model.) Idealized section through a continent–ocean–continent subduction zone. It shows the situation just after the oceanic crust was completely subducted and had been followed up to an assumed depth of *ca* 80 km by the downgoing marginal (thinned) continental crust. The displacement of marker point α will be followed during the successive steps of the model.

The initial stage (step 0)

The initial stage (Fig. 3) shows the evolution at the point where oceanic crust has been completely subducted and followed by continental margin crust to a depth of approximately 80 km. It corresponds to the setting before the first basement nappes formed in subducted continental crustal rocks. Subduction of continental margin crustal rocks without significant internal deformation or detachment is attributed to the following facts.

(1) A thin continental marginal crust. Thickness estimates between 10 (distal part) and 25 km for a 100–200 km wide Alpine-type marginal crust are supported by geological data (Roeder, 1989; Bernoulli *et al.*, 1990; Stampfli *et al.*, 1991; Favre and Stampfli, 1992).

(2) Low shear stress in the crust owing to the overlying very weak zone formed from the subducted accretionary prism.

(3) The subducted crust remained relatively cold because the isotherms were advected downwards (300°C isotherm to at least 40–50 km) by the subduction, as in oceanic subduction zones. This thermal regime is consistent with the high-pressure–intermediate-temperature metamorphic conditions seen in Alpine rocks buried at this stage. By implication, a large part of the subducting crust remained strong under brittle, high-pressure, low shear stress, conditions and did not undergo significant amounts of ductile strain.

(4) The negative buoyancy of the subducted oceanic slab allowed unconstricted subduction of the continental margin.

Figure 3 shows a schematic NW–SE section through the Western Swiss–Italian Alps in mid-Eoalpine time. The overriding plate is simplified by comparison with the Austroalpine cover and shows only three brittle thrust nappes of basement rocks (nappes SE1–SE3). These units, separated by thrusts A and B, are interpreted to have been formed at an early stage of subduction during the compressional break up of the southeastern (SE) continental margin. Both the SE1 and the SE2 thrust sheets were separated from their original southeastern crust (Adriatic upper plate) under relatively brittle conditions and later dragged down by the subducting oceanic crust.

In comparison to the Alps, the lower SE3 nappe may represent the Valpelline and the SE2 the Arolla-Sesia (Gneiss Minuti) nappe. The superposition SE3–SE2 could then correspond to the early Eoalpine thrusting of Valpelline on Arolla (Fig. 2). The SE1 nappe made of lower crust may be the equivalent of the IIDK zone. The Canavese zone and all the complications associated with its closure are not represented on Fig. 3. One could, however, tentatively correlate the main thrust A with the Canavese line.

THE FORMATION AND EARLY UPLIFT OF HIGH-PRESSURE METAMORPHIC BASEMENT NAPPES

The following model steps offer an explanation for the formation and subsequent uplift of high-pressure–intermediate-temperature rocks under compressional stress conditions. The model therefore differs from the extensional explanations proposed by Platt (1986), Ruppel *et al.* (1988) and Merle and Ballèvre (1992). On the other hand, it resembles more the mechanism proposed by

England and Wortel (1980), Malavieille (1995) and Chemenda *et al.* (1995) for the exhumation of rocks in the Himalayan central belt. However, the proposed combination of buoyancy forces and erosion in our model are not the principal causes for the uplift, although they may play an accessory role. The geological factors and published original ideas contributing to the mechanism proposed here are as follows.

(1) Although Neoalpine uplift and backfolding in the Alps are related to each other, the early (Eoalpine) upward movement of high-pressure rocks has taken place well before the onset of retro-movements, and thus by a different mechanism.

(2) Most originally deep basement rocks visible in outcrops display penetrative early schistosities and stretching lineations, implying a strong deformation throughout most of the rock volume. Consequently, it is unrealistic to represent large deep-seated rock bodies as having been displaced over significant distances without strong internal deformation.

(3) The extrusion mechanism proposed by Dietrich and Casey (1989), for the formation of Helvetic cover nappes by the combination of simple shear and heterogeneous wedge-shaped pure shear, may be applied also to basement fold nappes.

(4) Schmid *et al.* (1990) in the Eastern Alps propose a mechanism of viscous horizontal intrusion for the ductile refolding of deep basement nappes. The concept presented in our model is similar, except that the intrusion also has an important vertical component.

(5) Michard *et al.* (1993) concluded that the high-pressure coesite-bearing rocks of the Dora-Maira unit (southwest equivalent of the Monte Rosa nappe) underwent an early uplift under compressional conditions. Their proposed mechanism by a forced-return flow of imbricate slices, in an on-going subduction setting, is similar to that of our first stage, as described in the following pages.

First stage of nappe formation and uplift

Step 1 (Fig. 4) shows a conceptual set of processes that follow from a constriction or partial blockage in the continued subduction of the continental margin (Fig. 3). The constriction is considered to develop in the subduction channel below the main detachment zone, such that the upper continental crust to the northwest and above L–L′ no longer subducts at the same rate as the lower crust beneath it. The subduction channel refers to the zone above the lowest decoupling level in the subducting lithosphere and below the highest decoupling level in the mantle of the overriding plate. This definition represents a generalization from the small scale (e.g. Shreve and Cloos, 1986). The constriction or blockage can occur when any of the factors listed above that favour subduction without deformation in the initial stage (Fig. 3) are not sustained. In addition, the buoyancy of the continental crust in the subduction channel may balance the shear tractions on its bounding surfaces.

To simplify the discussion, L–L′ (Fig. 3) is taken to represent a material line in the subduction channel where the blockage has reduced the velocity at L to zero. Subduction continues (Fig. 4, Step 1a) by decoupling beneath the blocked upper continental crust, essentially along a zone of active simple shear at its base. The thickness of *ca* 4 km of this active shear zone at the base of the embryonic nappe was chosen to resemble existing basal shears in basement nappes. Continued convergence, shown here after 30 km, creates a thick embryonic nappe. Note that to simplify the model the simple shearing of L–L′ is mainly restricted to the decoupling zone at its base.

Although a downward dimpling of the subducting plate is shown to accommodate underthrusting and thickening of the nappe pile (Fig. 4, Step 1a), the flexural strength of the subducting lithosphere will both resist this deformation and redistribute it at a larger (flexural) wavelength. An equivalent upwarp will be resisted by the stronger overriding mantle. Decoupling and simple shearing can, however, continue if the embryonic nappe is also synchronously squeezed and flattened by ductile pure shear (Step 1b). Again, this is envisaged to be a dynamical process in which the strength of the nappe and resistance to shear on its boundaries compete with the resistance to vertical displacement of the footwall and hanging wall. Given current concepts of the controlling rheologies and associated densities of mantle (olivine) and upper crust (quartz), flattening may be the dominant effect, particularly when the hanging wall is the strongest part of the mantle lithosphere. Given that L remains stationary and that L′ is only displaced by the simple-shear component, and assuming constant volume and stretching in the plane of section, the result of flattening will be the upward expulsion or intrusion of the escaping ductile nappe NW1. L–L′ is in this case the 'pin-line' for the pure-shear flow component.

In Fig. 4 (Step 1b) the oblique escape up the subduction zone leads to the intrusion of nappe NW1 into the weaker accretionary prism. Flattening and intrusion enhances the basal simple shear and the combination of simple and pure shear creates a fold nappe of the Monte-Rosa type by a mechanism that is similar to that envisaged by Dietrich and Casey (1989) for some Helvetic cover nappes and the refolding of Eastern Alpine basement nappes (Schmid *et al.*, 1990). Buoyancy forces assist the intrusion but are not the dominant factor.

In Step 1c (Fig. 4) the effect of isostatic adjustment is added to account for the thickening of the nappe pile that was not offset by flattening. The main effect is to flex the pro-lithosphere downward and for the flexural/subduction hinge to migrate pro-ward together with the main pro-flysch basin.

If it is accepted that the three processes of Fig. 4 are synchronous, the vertical component of uplift of the

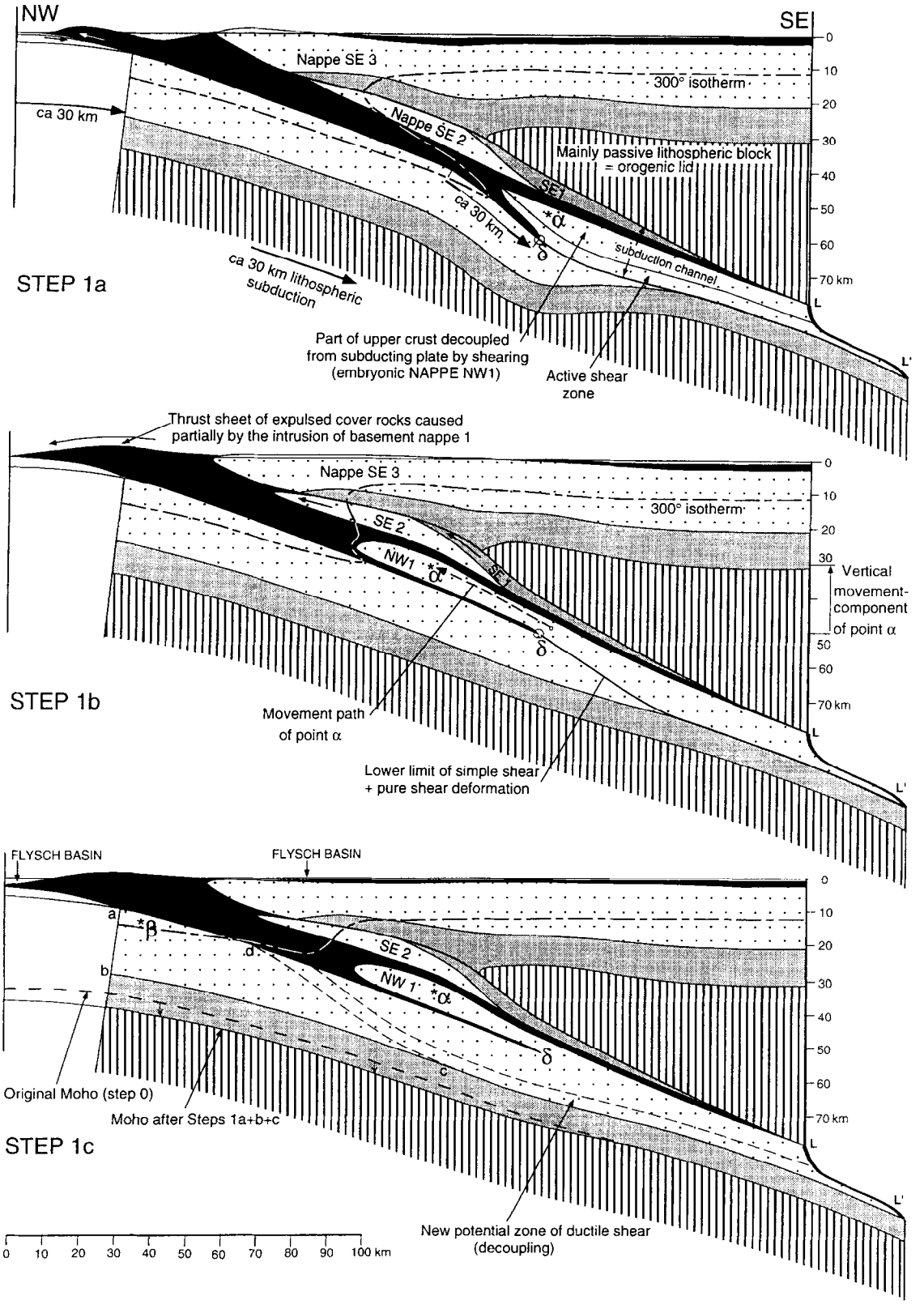

Fig. 4. (Step 1 of the model.) Situation after *ca* 30 km of lithospheric material has been subducted in continuation to the initial stage of Step 0 (Fig. 3). The three main mechanisms active during this stage are shown separately, even if in reality they probably have acted almost simultaneously. Step 1a—formation of an hypothetical embryonic NW1 nappe by heteregeneous simple shear along a shallow dipping (*ca* 20°) active zone of decoupling. Step 1b—superimposed heterogeneous pure shear, and intrusion of nappe NW1. Attenuation of the preceding buckling of the lower crust and mantle. Some separation of the hanging walls and footwalls takes place during the intrusion. Nappes SE1 and SE2 are also slightly flattened and moved upwards. Step 1c—approximate isostatic adjustment and resulting displacement to the northwest of the subduction hinge and the flysch basin. The 300°C isotherm is approximately equilibrated.

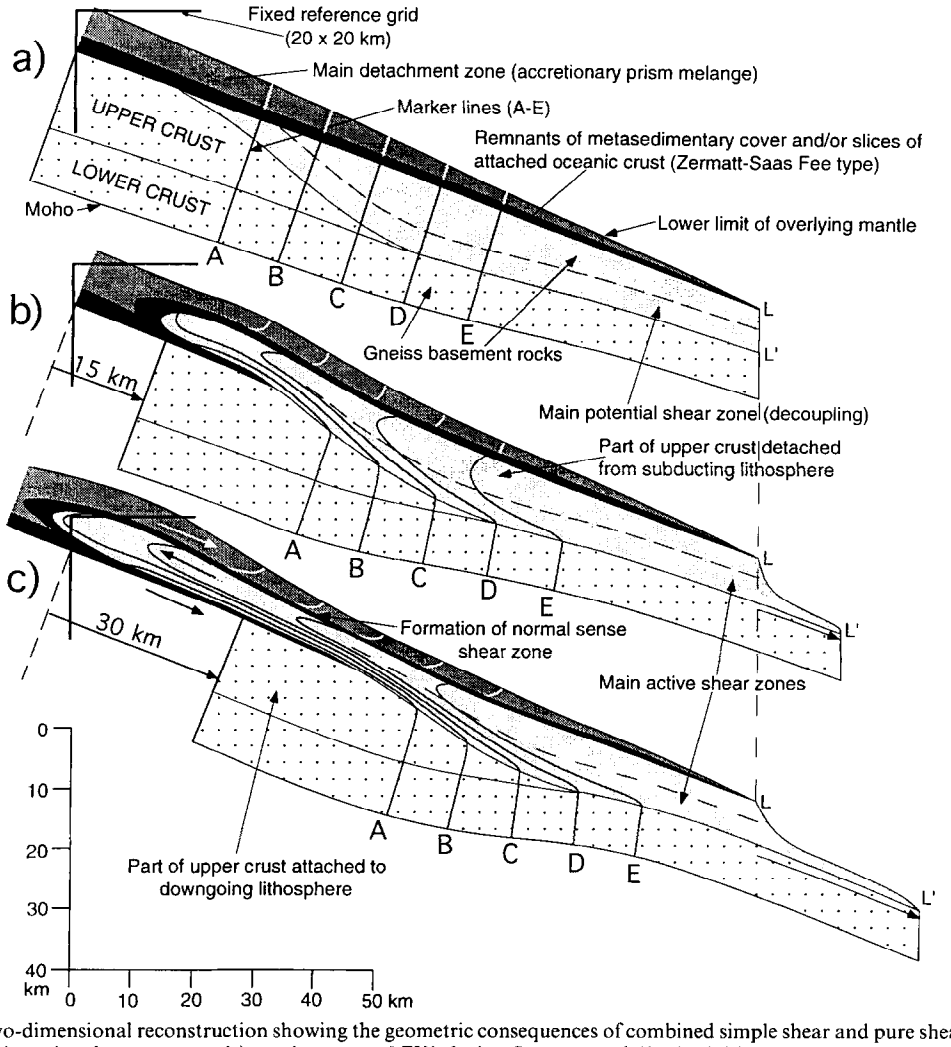

Fig. 5. Two-dimensional reconstruction showing the geometric consequences of combined simple shear and pure shear in the system envisaged to have generated intrusion nappe NW1 during Steps 1a and 1b. An initial stage (a) is followed by two progressive stages of deformation (b and c), each corresponding to a lithospheric subduction of 15 km. For further explanation see the text.

frontal nose of the nappe (20 km, from 45 to 25 km approximately; Fig. 4b) occurs in the same time span that convergence/subduction consumes 30 km of lithosphere, which is 1–6 Ma for subduction velocities between 3 and 0.5 cm/year. These rates meet the important requirement that the nappe be expelled upward faster than the general rate of thermal equilibration in a subduction zone setting. The nappe would tend to cool as it intrudes the higher cooler part of the subduction complex and preserve the high-pressure–intermediate-temperature metamorphism. The effect of intrusion is also to place the high-pressure rocks in contact with the overlying lower pressure schists of the accretionary prism (the Tsate nappe in the Alpine context) along a low-angle 'normal fault' but in a tectonic setting without any net extension of the overall system.

The geometry and scale of nappe NW1 during the early stages of Step 1 correspond to the P–T conditions of the Monte Rosa high-pressure rocks (*ca* 15 kbars, 500°C) but would vary during the evolution of a given orogen. Some thermal re-equilibration has been included in the nappe, and conditions at the end of Step 1c are thought to correspond to the Eoalpine metamorphic temperature peak in the Western Swiss–Italian Alps at 85 Ma (Fig. 2).

In reality it is likely that the blockage at point L is only temporary. However, as long as L moves more slowly downwards than the upward velocity imparted by flattening, the result will still be an intrusion-type nappe, although with a lower uplift velocity.

Geometry of the nappe intrusion mechanism

A geometrical two-dimensional construction (Fig. 5) illustrates the sequential evolution of nappe NW1 (Fig. 4) through steps (a)–(c) that combine the simple- and pure-shear deformations described above. The reconstruction follows some simple rules: (1) cross-sectional areas are conserved; (2) viscous (ductile) deformation is restricted to the nappe and is focused in the shear zone at its base; (3) the overlying weak fluid-rich accretionary mélange is

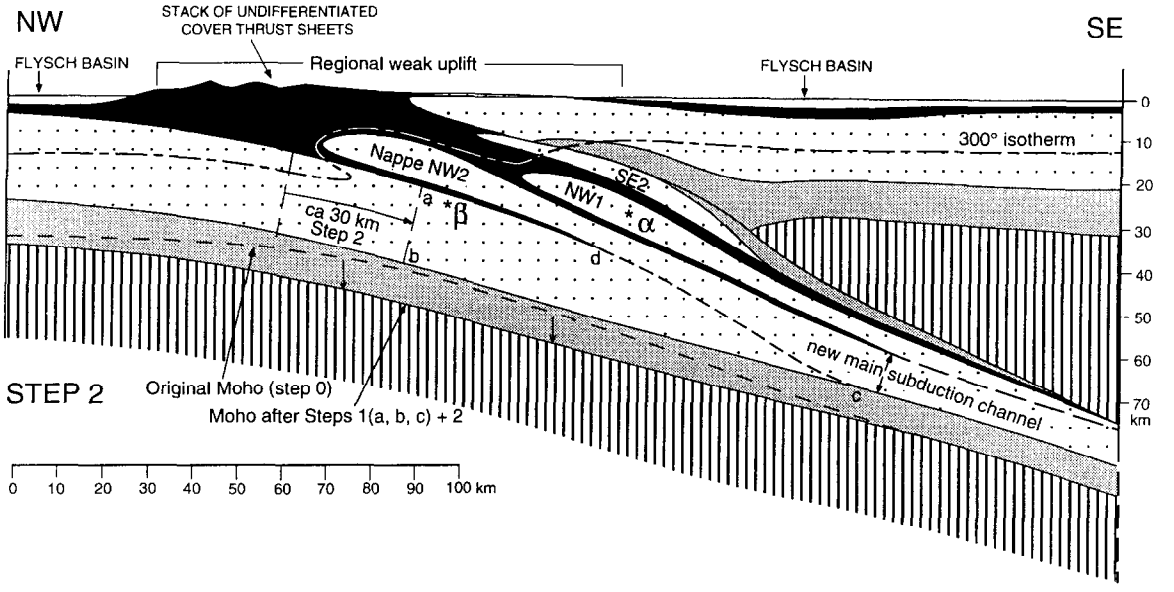

Fig. 6. (Step 2 of the model.) Formation of a new intrusion-type nappe (NW2) after a further 30 km of lithosphere has been subducted. The upper crustal area *abcd* of Step 1c moved down *ca* 30 km. The same rules and mechanisms which created the preceding nappe NW1 are incorporated here too. A new marker point β is introduced.

assumed to form a low friction normal fault contact with the upward moving nappe; (4) a small increase in the thickness of the subduction channel, and nappe pile, owing to footwall and or hanging wall deformation is included; and (5) downward velocity of the nappe is assumed to be locally zero at L, possibly as a consequence of the superimposed upward velocity due to flattening.

The model corresponds largely to the mechanism of wedge-shaped pure shear (Ramsay and Huber, 1987, p. 620), and is characterized by a cumulative effect in the frontal part of the nappe. This makes it possible to obtain high uplift values during a restricted time span. The amount of internal finite strain and relative uplift (intrusion) depends on several factors which can be investigated in numerical models. The primary controls are the strength of the nappe and the resistance to the widening of the subduction channel. The mechanism is considered to be valid in a conceptual sense and the geometry has been chosen to show how the mechanism would have to operate to produce existing basement fold nappes, particularly Monte Rosa-type nappes. In this regard, the simple geometrical construction is in agreement with the following observations.

(1) The inverted flank is strongly deformed with two-dimensional finite-strain ellipse values of E_{xx}/E_{yy} between 30 and 60, while the central part and normal limb are much less deformed ($E_{xx}/E_{yy} = 2$–8).

(2) The root zone of the nappe becomes more thinned than its frontal part.

(3) The rocks attached as cover to the basement (metasediments, slices of oceanic crust) are finally found surrounding the fold structure. This may explain the present position of the high-pressure Zermatt-Saas Fee and Antrona units, folded around the frontal part of the Monte Rosa nappe (Fig. 1).

(4) The contact between the inverted limb and the underlying units corresponds to a low-angle thrust.

(5) The contact between the normal limb and the overlying units appears, on the contrary, as a low-angle 'normal fault', comparable to the Combin fault.

It is probable that the proposed mechanism could produce high-pressure intrusion nappes from almost any depth along an active subduction channel.

Formation and possible uplift of subsequent nappes

The same mechanism may operate to form subsequent basement fold nappes as shown conceptually in Fig. 6. The new fold nappe (NW2) is situated in a more external position and was created using a new shear zone below and in front of NW1 (Fig. 4, Step 1c). NW1 is supposed here to be entirely detached from the subducting rocks (Fig. 6). NW2 is larger than NW1 because the continental margin crust involved is assumed to be thicker. It is also assumed that: (1) nappes NW1 and SE2 may be further flattened and intruded upwards as NW2 is formed; (2) the same isostatic mechanism causes the subduction hinge and flysch basin to migrate to the northwest; and (3) the overall thickening and isostatic balance begins to cause a weak regional uplift of a few km. In the southeast this could correspond to the first weak retro-movements that are precursors to the major backfolding of the collision phase.

In comparison to the Western Swiss–Italian Alps, the most likely equivalents for nappes of the NW2 type are the Mont Fort and Siviez-Mischabel nappes (Figs 1 and 2). Step 2 could in that case correspond to a time span between the Late Paleocene and the Early Oligocene (Mesoalpine).

FORMATION OF DOUBLY-VERGENT STRUCTURES AND LATE-STAGE UPLIFT OF EARLIER NAPPES

The late-stage collisional evolution of most orogens, and the Alps in particular, is characterized by both pro- and retro-movements, the latter leading to backfolding and thrusting and the development of the doubly-vergent style described earlier. In the Western Swiss–Italian Alps only N- to W-vergent pro-structures were formed prior to the activation of retro-structures in the Middle Oligocene, which in turn signal the onset of Neoalpine events (Fig. 2). NW-vergent nappes continued to form and a generalized uplift of the Alpine range took place accompanied by molasse sedimentation in both the northwest and southeast peripheral foredeep (foreland) basins.

Mechanism of simultaneous pro- and retro-shear movements

The geodynamical models (Beaumont *et al.*, 1996) indicate that the change to doubly-vergent tectonics follows from a reduction in the convergent material that can be accommodated by the subduction channel. Both sandbox (Malavieille, 1984; Malavieille *et al.*, 1993; Larroque *et al.*, 1995) and numerical experiments (Willett *et al.*, 1993; Beaumont *et al.*, 1994) show that conjugate pro- and retro-deformation occurs in a crustal layer that is forced to deform by the subduction of the underlying pro-lithosphere. The conjugate deformation occurs in the part of the layer that does not subduct (Figs 1–5) (Beaumont *et al.*, 1994).

By implication, something occurred in the Alps in the Middle Oligocene to choke off the subduction of pro-crust of the European margin. The most simple explanation is a reduction of the negative slab load which acted to flex the pro-lithosphere upwards and to close the subduction channel. Two possible mechanisms are the 'break off' of the subducted slab and/or the increase in buoyancy as progressively more low-density continental lithosphere enters the subduction zone. The former mechanism would probably lead to a more rapid change in tectonic style, whereas the latter would be related to the properties of the continental margin and the convergence velocity.

Figure 7 shows how the basic doubly-vergent style of the numerical models can be used in the context of the geometrical evolution of Alpine-type basement nappes. As in the preceding steps, the geometric effects of simple shear, pure shear and isostatic adjustment are examined separately under the assumption that cross-sectional area is conserved and motion occurs in the plane of the profile. Figure 7(a) shows a simplified form of the initial geometry when the conjugate pro- and retro-shears (Z1 and Z2, respectively) connecting to the basal shear (Z3) are first activated. Their relationship to the existing model nappe pile is shown in Fig. 8(a). Point d corresponds to the subduction detachment or stress singularity (Willett *et al.*, 1993) retroward of which the crust and upper mantle are stationary unless involved in retro-charriage. This implies that because the subduction channel above Z3 has now been blocked, crust that is decoupled to form the nappe NW3 above shear Z1 will later be carried in the hanging wall of Z2 and not partly subducted in the hanging wall of Z3, which was the tectonic style of the earlier subduction phase.

Figures 7 and 8 show the geometrical evolution based on the numerical model results but adapted for a crustal section that dips retroward (Fig. 7), and in which pro-crust is detached as discrete slices to form nappes and not continuously as in the numerical models. The discrete nature of the shear zones means that the pro-shear, Z1, will move with the pro-crust that contains it while the point c (Figs 7a and 8a & b) moves toward d. The geometry after 40 km of convergence (Fig. 7b) has been constructed assuming an equal 20 km conjugate simple shearing on Z1 and Z2, and the full 40 km finite offset on Z3 with most of the deformation confined to the simple shear zones. It shows two fold structures, one pro- and one retro-oriented. Additional contributions from heterogeneous pure shear and isostatic adjustment are added in Fig. 7(c & d). The construction is similar to that used in Fig. 5 but with smaller amounts of pure shear strain. Even though there is no fundamental difference between the pro- and retro-structures, the former are newly formed nappes, whereas the latter refold earlier formed nappes (Fig. 8b, Step 3).

The approximately 20° retroward dip of the entire system causes a general downward absolute motion of most rocks in the pro-nappe, while the majority of those of the retro-structure move upwards and will approach the surface if there is erosion (Fig. 7d). This may explain why NW-vergent nappes in the Alps are mostly characterized by prograde metamorphism, while the large Alpine backfolds are associated with retrograde metamorphism and uplift.

Finally, in the continuum numerical models the triangular region between the bounding Z1 and Z2 shears acts as a relatively undeforming plug that is carried retroward in the hanging wall of Z2 (Willett *et al.*, 1993). The effect of discrete, as opposed to continuous, detachment of pro-crust may modify this behavior. For example, if the nappes continue to undergo pure-shear flattening as described for Steps 1 and 2, brittle rocks in their hanging wall in the central part of the orogen may be affected by normal faults. This concept has not been tested with numerical models.

Late orogenic synchronous pro- and retro-shear movements

Step 3 (Fig. 8b) illustrates the formation of the pro-nappe NW3 and the synchronous backfold. NW3 is added to the pro-wedge nappe stack, slightly uplifting NW2, whereas the backfold refolds and partly uplifts the previously formed internal units (nappes SE1–SE3 and

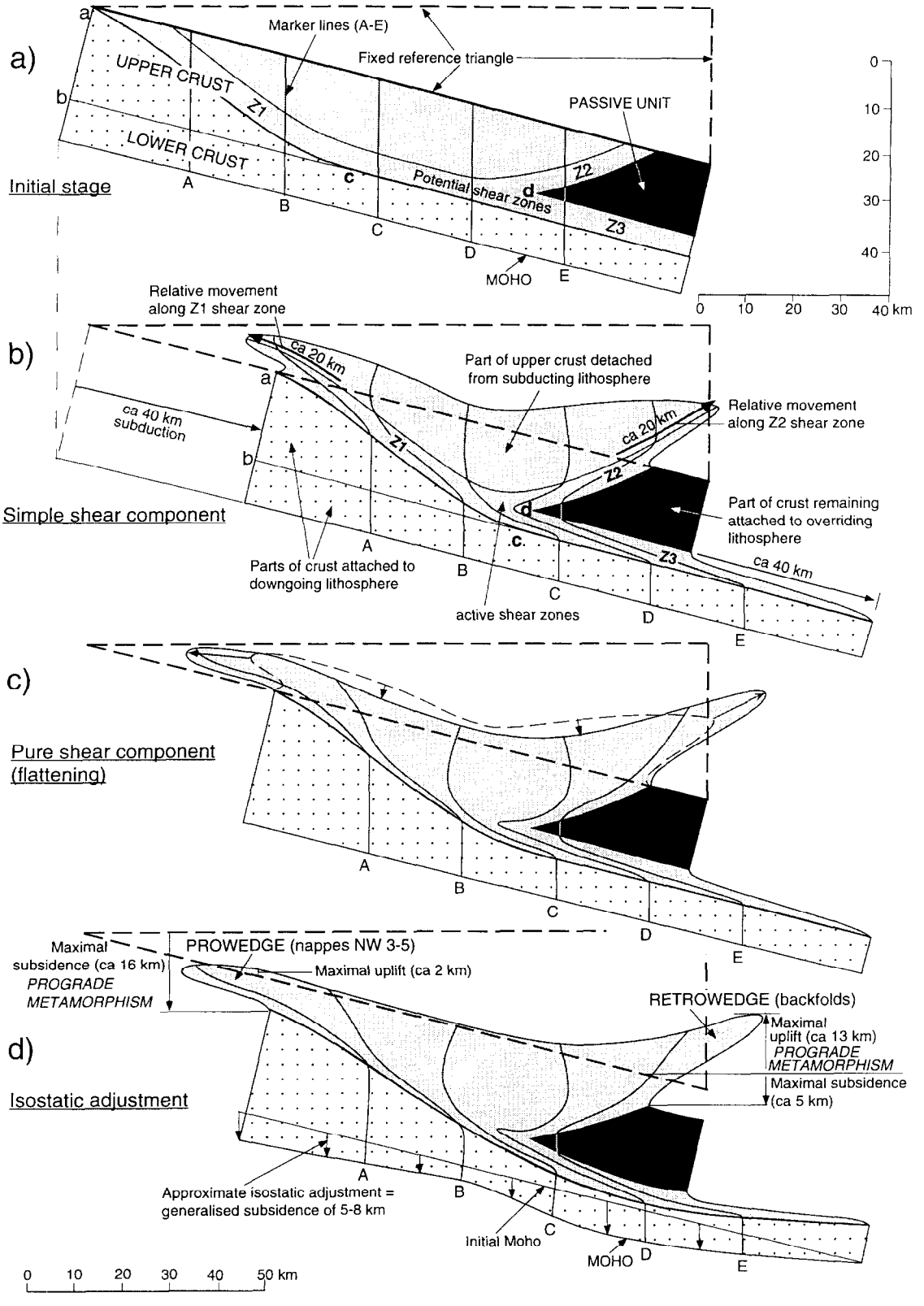

Fig. 7. Two-dimensional model proposed for the simultaneous formation of pro- and retro-structures (doubly-vergent) during continuing lithospheric subduction. All deformation is supposed to have taken place within the plane of the section. (a) Initial situation with the creation of a new system of potential detachment zones by ductile shear, including for the first time a retro-shear zone (Z2). (b) Situation after 40 km of lithospheric subduction has been accommodated by simple shear along the active Z1, Z2 and Z3 zones. The amount of finite shear strain and displacement is arbitrarily chosen to be equal along Z1 and Z2. (c) Pure shear strain is superposed on the preceding geometry. The two-dimensional flattening component in both pro- and retro-folds can be represented by a finite-strain ellipse with a value $E_{xx}/E_{yy} = ca\ 2$. (d) An approximate isostatic adjustment of the system corresponds to a subsidence varying between 5 and 8 km.

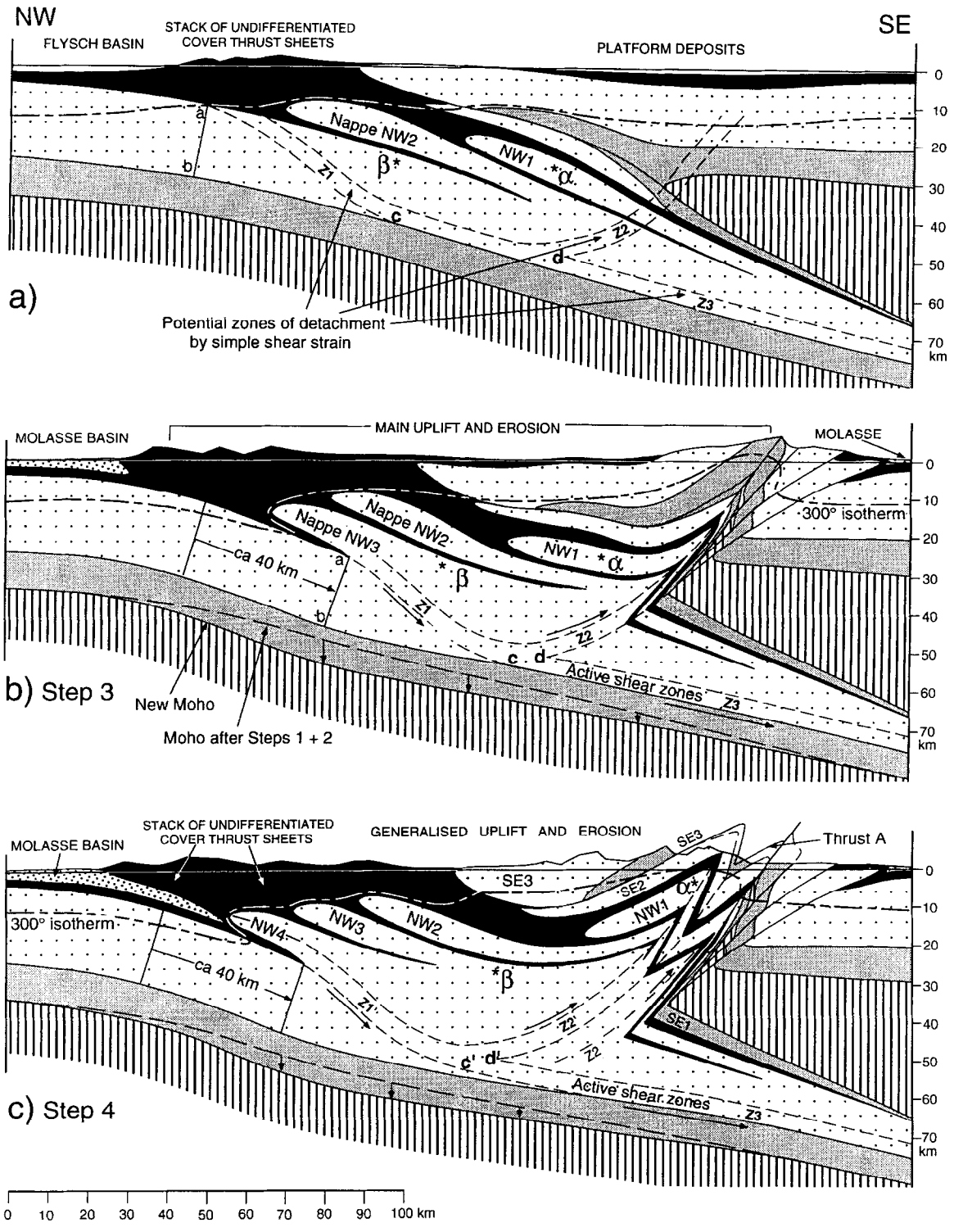

Fig. 8. The formation of simultaneous NW-vergent (pro-) and SE-vergent (retro-) folds and thrusts, and the generalized uplift of the system, during three successive steps corresponding each to *ca* 40 km of lithospheric subduction. (a) Initial stage in relation to the first retro-movements. It is identical to Fig. 6 except for the 300°C isotherm, which is assumed to have risen by thermal equilibration, and the sealing of the subduction channel owing to the increased buoyancy of the subducting lithosphere. (b) (Step 3 of the model.) Formation of pro-fold nappe NW3 along shear zone Z1, and synchronous retro-folding and thrusting along Z2, using the mechanism of Fig. 7. The location of Z2 is probably controlled by the overlying (southeast) lithospheric mantle. (c) (Step 4 of the model.) Creation of one more pro-nappe (NW4) at the same time as one additional retro-structure along shear zone Z2'.

NW1). The upper portion of the retro-movements is shown occurring on discrete thrust surfaces (Fig. 8b) because the upper part of the crust, above the 300°C isotherm, and probably the upper mantle are brittle. These stacking movements elevate the internal part of the belt. Simultaneously the external (pro-) region is uplifted by the 40 km of cover rocks that were stripped from their basement to create Alpine relief, erosion and continental sediment (molasse). The thickening of the crust also caused isostatic subsidence and flexural migration of the pro-foreland basin to the northwest.

This process of discrete detachment of slices of the pro-crust, formation of basement nappes, nappe stacking and retroward backfolding can be expected to repeat itself. Certainly when c (Fig. 8a) reaches d (Fig. 8b) a more external pro-shear (Z1′) develops (Fig. 8c) if attached pro-crust is not to underthrust d and subduct.

When compared with the Western Swiss–Italian Alps, the last-formed pro-nappes (NW3–NW5; Fig. 8) are the equivalents of the Mont Blanc, Aiguilles Rouges and Infra Rouges nappes. The geometry of the retro-side of the system (Fig. 1) indicates that similarly several discrete retro-shears (Z2, Z2′ annd Z2″, Fig. 9) developed with their positions migrating to the northwest even though the general direction of material transport is to the southwest. The effect of these successive discrete retro-shears is shown geometrically (Fig. 9) and, in the context of the Alps, Z2, Z2′ and Z2″ correspond best to the Boggioletto, Vanzone and Berisal structures.

Development of several successive retro-shears can be understood geometrically to require associated movements of d. In the numerical models pro-ward stepping of d follows from retrograde migration of the subducting slab, loosely termed slab retreat or rollback. Alternatively, the detachment depth in the pro-crust may become progressively shallower as each pro-nappe is formed. This would cause a corresponding upward stepping of d and generate a nested set of pro- and retro-structures in which each successive conjugate pair of shears (Z1 and Z2, Figs 8 and 9) would be positioned at a higher level and in a more proward position. A third possibility is that d remains stationary, that the subsidiary retro-shears are paired with corresponding subsidiary pro-shears and together they represent a succession of bounding shears on triangular block uplifts located at the pro-ward end c of the basal shear zone (Fig. 7a) during each cycle of nappe formation.

CONCLUSIONS

Even if our model includes only one oceanic subduction zone, the final two-dimensional geometry after Steps 1–5 (Fig. 9) displays many of the same basic characteristics as those of the Western Swiss–Italian Alps shown on the profile in Fig. 1. Although this is partly the consequence of the geological constraints applied to the model, it still indicates that the proposed mechanism of nappe formation and stacking is possible.

Tectonic stages

Three main tectonic stages during the Alpine-type convergent movements are distinguished and each can be correlated with the formation of specific nappe structures.

(1) The initial stage (Step 0) of our model represents the situation after the formation of brittle Austroalpine-type basement thrust sheets (nappes SE1–SE3) and the subduction of oceanic crust, followed by at least 180 km of thinned marginal continental crust. The early Eoalpine SE1–SE3 basement thrust nappes are interpreted to have

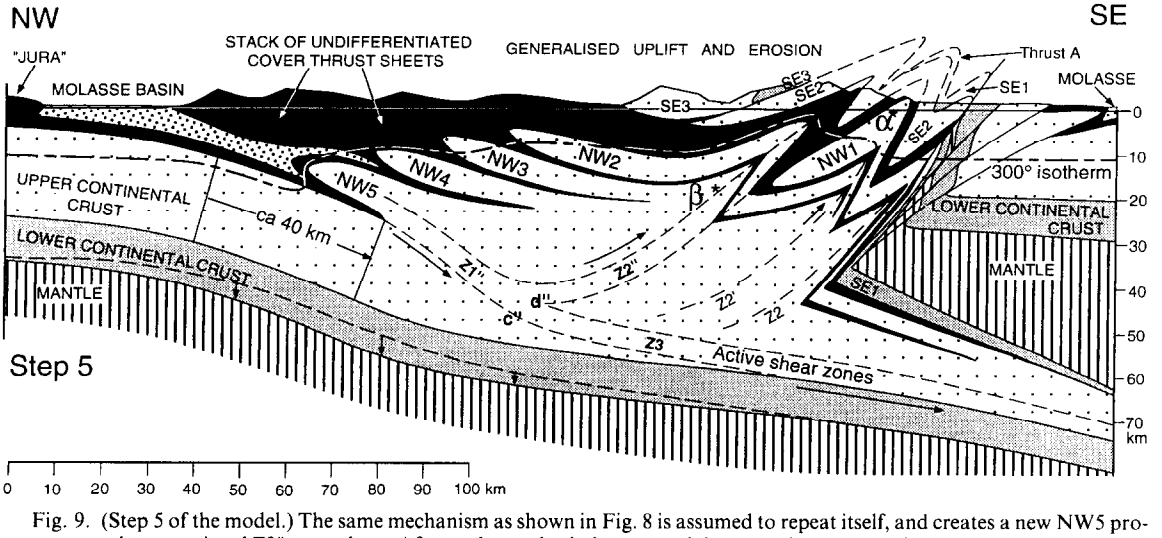

Fig. 9. (Step 5 of the model.) The same mechanism as shown in Fig. 8 is assumed to repeat itself, and creates a new NW5 pro-nappe and an associated Z2″ retro-shear. After each step, both the pro- and the retro-shear zones migrated to the northwest. At the same time point d moved to the northwest and upwards. Step 5 is assumed to represent a late to final stage in the crustal collision.

been formed at an early stage of oceanic crust subduction during the compressional breakup of the southeastern continental margin. All structures formed during the initial stage are single (NW) vergent.

(2) The second stage corresponds to the partial and, probably, temporary blockage of subducting upper continental crust below a depth of 70 km. This initiated the formation and subsequent uplift of high- to medium-pressure basement fold nappes under compressional conditions. These structures are equivalent to the Late Eoalpine and Mesoalpine nappes derived from the internal Briançonnais continental crust. The second stage gives a possible explanation for the subduction to more than 50 km depth and the following rapid uplift and decompression above 30 km of high-pressure rocks. This is shown in a simplified way in Fig. 10 by the movement path of marker point α contained in nappe NW1 during Steps 0–2. As during the first stage, all structures formed are single (NW) vergent. The second stage (Steps 1 and 2) corresponds to a minimal crustal shortening of 60 km.

(3) The third stage is characterized by the total blockage of most of the subducting upper continental crust. This resulted in a doubly-vergent style with both pro- and retro-movements. The former created NW-vergent basement nappes, as seen in the external Alpine massifs, and the latter caused backfolding and thrusting, typical of the internal Alps. This third stage corresponds to the Neoalpine movements in the Western Swiss–Italian Alps, and is accompanied by a generalized uplift, erosion and molasse sedimentation. The limited downward movement of marker point β (Fig. 10) up to Step 3, is representative of the general rock motion in the pro-nappes, while the paths of α and β (Steps 3–5) show the general upward motion during retro-movements. The minimal crustal shortening during the third stage amounts to *ca* 120 km.

Compared to the results of numerical modeling by Beaumont *et al.* (1996), our initial stage is equivalent to phase 1 (subduction of oceanic lithosphere) and early phase 2 (partial subduction of continental margin), and our second stage corresponds best to late phase 2. Finally, our third stage is identical to phase 3 (collisional orogen) of the numerical model.

Burial, uplift and decompression

One of the consequences of the proposed model is that large portions of continental crust were subducted at great depth during the first two stages. Part of these crustal rocks continued to be subducted, while probably only a fraction underwent uplift and participated to the building of high- to medium-pressure nappes. According to the model, the high-pressure intrusion nappes moved upwards (with decompression) at rates of between 3 and 20 mm/year during the second stage, and at lower rates of 1–4 mm/year during the third stage (Fig. 10).

During the collisional third stage, however, most of the upper crust did not reach more than 30 km depth and its major portion contributed to the development of late pro- and retro-structures. This main difference is confirmed by the significant amount of time (40–50 Ma) that was necessary to create the Eo- and Mesoalpine deep nappes, whereas the later shallower nappes and backfolds took only *ca* 20 Ma to be formed.

Crustal shortening

The model shows how a shortening of at least 360 km of continental crust is needed, following the closure of the oceanic domain, to produce a total of five basement nappes (NW1–NW5). In the Alpine collision, where at least two oceanic lithospheres were subducted and many

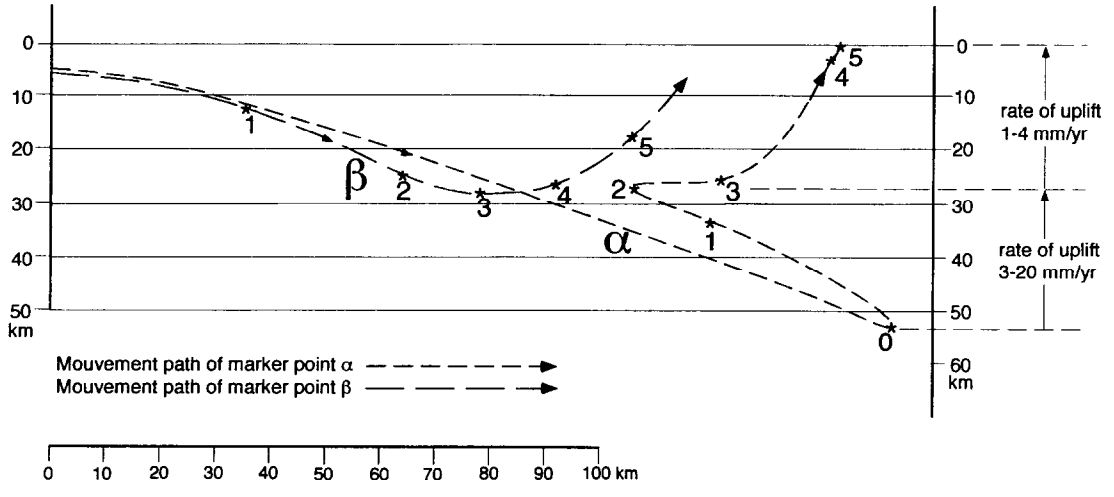

Fig. 10. Movement paths of marker points α and β during Steps 0–5. Point α is situated in nappe NW1 and its path represents rock displacement during the early stage of deep subduction and uplift (Steps 0–2), followed by later uplift during retro-movements (Steps 3–5). The path of β (situated near nappe NW3) corresponds to rock movement during the last stage of pro- and retro-deformation. It shows how the same rocks followed a relatively shallow downwards movement in the pro-wedge (Steps 1–3) directly followed by an uplift in the retro-wedge (Steps 4 and 5). The rate of vertical upward movement during Steps 1 and 2 for point α is of the order of 3–20 mm/year. The rate of later uplift during Steps 3–5, for both points α and β is of the order of 1–4 mm/year. These values are valid for crustal subduction velocities between 0.5 and 3 cm/year.

more nappes were formed than in our model, the shortening must have been considerably more important.

Acknowledgements—We thank very much Jean-Luc Epard, Marc Escher, Jean Guex, Michel Jaboyedoff, Juliet Hamilton, Johannes Hunziker, Michel Marthaler, Henri Masson, Robin Marchant, Jon Mosar, Mario Sartori, Gérard Stampfli, Stefan Schmid and Albrecht Steck for discussions, help and encouragement. Constructive critical reading of the manuscript by Jean-Pierre Burg, C. W. Passchier and Adrian Pfiffner is gratefully acknowledged. We thank the Swiss National Science Foundation (grants 21.31082.91 and 20.37470.93) for their financial support.

REFERENCES

Argand, E. (1911) Les nappes de recouvrement des Alpes Pennines et leurs prolongements structuraux. *Matériaux Carte géologique Suisse (n.s.)* **31**, 26.

Argand, E. (1916) Sur l'arc des Alpes Occidentales. *Eclogae Geologicae Helvetiae* **14**, 145–191.

Argand, E. (1934) La zone pennique. In *Guide Géologique de la Suisse, Vol. 3: Introductions Générales*, pp. 149–189. Wepf & Co., Basel.

Ayrton, S., Bugnon, C., Haarpainter, T., Weidmann, M. and Frank, E. (1982) Géologie du front de la nappe de la Dent Blanche dans la région des monts Dolins, Valais. *Eclogae Geologicae Helvetiae* **75**, 269–286.

Badoux, H. (1962) Géologie des Préalpes valaisannes. *Matériaux Carte géologique Suisse (n.s)* **11**, 1–86.

Barnicoat, A. C., Bowtell, S. A. and Cliff, R. A. (1991) Timing of high-pressure metamorphism in the Zermatt-Saas zone, Switzerland. *Terra Abstracts* **3**, 89.

Barnicoat, A. C. and Fry, N. (1986) High-pressure metamorphism of the Zermatt-Saas ophiolite zone, Switzerland. *Journal of the Geological Society of London* **143**, 607–618.

Bearth, P. (1952) Geologie and Petrographie des Monte Rosa. *Beiträge zur Geologischen Karte Schweiz. (N.F.)* **96**, 1–94.

Bearth, P. (1967) Die Ophiolite der Zone von Zermatt-Saas. *Beiträge zur Geologischen Karte Schweiz (N.F.)* **132**, 130.

Beaumont, C., Ellis, S., Hamilton, J. and Fullsack, P. (1996) Mechanical model for subduction—collision tectonics of Alpine-type compressional orogens. *Geology* **24**, 675–678.

Beaumont, C., Fullsack, P. and Hamilton, J. (1994) Styles of crustal deformation in compressional orogens caused by subduction of the underlying lithosphere. *Tectonophysics* **232**, 119–132.

Beaumont, C. and Quinlan, G. (1994) A geodynamic framework for interpreting crustal scale seismic reflectivity patterns in compressional orogens. *Geophysical Journal International* **116**, 754–783.

Bernoulli, D., Bertotti, G. and Froitzheim, N. (1990) Mesozoic faults and associated sediments in the Austroalpine–South Alpine passive continental margin. *Memorie della Società Geologica Italiana* **45**, 25–38.

Bertolani, M. (1968) La petrografia della Valle Strona (Alpi Occidentali Italiane). *Schweizerische Mineralogische Petrographische Mitteilungen* **48**, 695–732.

Blake, M. C., Fudral, S. and Roure, F. (1980) Relations structurales entre le massif de Lanzo et le massif de Sesia dans la région de Lanzo. Alpes occidentales, Italie. *Bulletin de la Société Géologique de France* **22**(1), 145–150.

Caby, R. (1981) Le Mésozoïque de la zone du Combin en Val d'Aoste (Alpes graies): imbrications tectoniques entre séries issues des domaines pennique, australpin et océanique. *Géologie Alpine* **57**, 5–13.

Chemenda, A., Mattauer, M., Malavieille, J. and Bokun, A. (1995) A mechanism for syn-collisional deep rocks exhumation and associated normal faulting: Results from physical modeling. *Earth and Planetary Science Letters* **132**, 225–232.

Colombi, A. (1989) Métamorphisme et géochimie des roches mafiques des Alpes ouest-centrales (géoprofil Viège-Domodossola-Locarno). *Mémoires de Géologie de Lausanne* **4**, 216.

Colombi, A. and Pfeiffer, H. R. (1986) Ferrogabbroic and basaltic meta-eclogites from the Antrona mafic–ultramafic complex and the Centovalli–Locarno region (Italy and southern Switzerland) First results. *Schweizerische Mineralogische Petrographische Mitteilungen* **66**, 99–110.

Dal Piaz, G. V. (1976) Il lembo di ricoprimento del Pillonet, Falda Dent Blanche nelle Alpi occidentali. *Memorie Istituti Geologia e Mineralogia di Padova, Italia* **31**, 61.

Dal Piaz, G. V., Gosso, G. and Martinotti, G. (1971) La II zona diorito-kinzigitica tra la Valsesia e la Valle d'Ayas (Alpi occidentali). *Memorie della Società Geologica Italiana* **10**, 257–276.

Dal Piaz, G. V., Hunziker, J. C. and Martinotti, G. (1972) La zona Sesia-Lanzo e l'evoluzione tettonico-metamorfica delle Alpi nordoccidentali interne. *Memorie della Società Geologica Italiana* **32**, 1–16.

Debelmas, J., Oberhauser, R., Sandulescu, M. and Trümpy, R. (1980) L'arc alpino-carpathique. In *Géologie des Chaînes Alpines Issues de la Téthys*, eds J. Aubouin, J. Debelmas and M. Latreille, pp. 86–95. Mém. Bur. Rech. Géol. Minières **115**.

Dietrich, D. and Casey, M. (1989) A new tectonic model for the Helvetic nappes. In *Alpine Tectonics*, eds M. P. Coward, D. Dietrich and R. G. Park, pp. 47–63. Geological Society of London Special Publication **45**.

England, P. and Wortel, R. (1980) Some consequences of the subduction of young slabs. *Earth and Planetary Science Letters* **47**, 403–415.

Epard, J.-L. and Escher, A. (1996) Transition from basement to cover: a geometric model. *Journal of Structural Geology* **18**, 533–548.

Escher, A. (1988) *Structure de la nappe du Grand Saint-Bernard entre le Val de Bagnes et les Mischabel.* Rapport géologique, Service hydrologique et géologique national Suisse **7**.

Escher, A., Hunziker, J., Marthaler, M., Masson, H. Sartori, M. and Steck, A. (in press) Geologic framework and structural evolution of the Western Swiss–Italian Alps. In *Deep Structure of the Swiss Alps: Results of the National Research Program 20 (NRP 20)*, eds O. A. Pfiffner, P. Lehner, P. Heitzmann, S. Mueller and A. Steck, pp. 205–222. Birkhäuser, Basel.

Escher, A., Masson, H. and Steck, A. (1987) *Coupe Géologique des Alpes Occidentales Suisses.* Rapp. Géol. Serv. hydrol. géol. nat. Suisse **2**.

Escher, A., Masson, H. and Steck, A. (1993) Nappe geometry in the Western Swiss Alps. *Journal of Structural Geology* **15**, 501–509.

Favre, P. and Stampfli, G. (1992) From rifting to passive margin: the examples of the Red Sea, Central Atlantic and Alpine Tethys. *Tectonophysics* **215**, 69–97.

Frei, W., Heitzmann, P. and Lehner, P. (1990) Swiss NFP-20 program of the deep structure of the Alps. In *Deep Structure of the Alps*, eds F. Roure, P. Heitzmann and R. Polino, pp. 29–47. Mémoires de la Société Géologique de France, Paris **156**.

Frey, M., Hunziker, J. C., O'Neil, J. R. and Schwander, H. W. (1976) Equilibrium–disequilibrium relations in the Monte Rosa granite, western Alps: petrological, Rb–Sr and stable isotope data. *Contributions to Mineralogy and Petrology* **55**, 147–179.

Ganguin, J. (1988) Contribution à la caractérisation du métamorphisme polyphasé de la Zone de Zermatt-Saas Fee. Ph.D. thesis, ETH Zürich.

Gerlach, H. (1869) Die Penninischen Alpen. *Denkschrift schweizer naturforschendes Gesellschaft* **23**, 1–68.

Handy, M. R. (1989) Deformation regimes and the rheological evolution of fault zones in the lithosphere: the effects of pressure, temperature, grain size and time. *Tectonophysics* **163**, 119–152.

Handy, M. R. (1990) The solid-state flow of polymineralic rocks. *Journal of Geophysical Research* **95**, 8647–8661.

Handy, M. R. and Zingg, A. (1991) The tectonic and rheological evolution of an attenuated cross section of the continental crust: Ivrea crustal section, southern Alps, northwestern Italy and southern Switzerland. *Bulletin of the Geological Society of America* **103**, 236–253.

Heim, Alb. (1921) *Geologie der Schweiz. Bd. II. Die Schweizeralpen.* Jauchnitz, Leipzig.

Heitzmann, P., Frei, W., Lehner, P. and Valasek, P. (1991) Crustal indentation in the Alps: an overview of reflexion seismic profiling in Switzerland. In *Continental Lithosphere: Deep Seismic Reflexions*, eds R. Meissner, L. Brown, H.-J. Dürrbaum, W. Franke, K. Fuchs and F. Seifert, pp. 161–176. American Geophysical Union, Geodynamic Series **22**.

Hermann, F. (1937) *Carta geologica delle Alpi Nord-Occidentali.* Uff. Cartographico, Milano.

Hitz, L. and Pfiffner, O. A. (1994) A 3D crustal model of the eastern external Aar massif interpreted from a network of deep seismic profiles. *Schweizerische Mineralogische Petrographische Mitteilungen* **74**, 405–420.

Hunziker, J. C. (1970) Polymetamorphism in the Monte Rosa, western Alps. *Eclogae Geologicae Helvetiae* **63**, 151–161.

Hunziker, J. C. (1974) Rb–Sr and K–Ar age determinations and the

Alpine tectonic history of the Western Alps. *Memorie Istituti Geologia e Mineralogia di Padova, Italia* **31**, 1–54.

Hunziker, J. C. and Martinotti, G. (1984) Geochronology and evolution of the western Alps. *Memorie della Società Geologica Italiana* **29**, 43–56.

Hunziker, J. C., Desmons, J. and Hurford, A. J. (1992) Thirty-two years of geochronological work in the Central and Western Alps: a review on seven maps. *Mémoires de Géologique de Lausanne* **13**, 1–59.

Hunziker, J. C., Desmons, J. and Martinotti, G. (1989) Alpine thermal evolution in the central and the western Alps. In *Alpine Tectonics* eds M. P. Coward, D. Dietrich and R. G. Park, pp. 353–367. Geological Society of London Special Publication **45**.

Hurford, A. and Hunziker, J. C. (1989) A revised thermal history for the Gran Paradiso massif. *Schweizerische Mineralogische Petrographische Mitteilungen* **69**, 319–329.

Lacassin, R. (1987) Kinematics of ductile shearing from outcrop to crustal scale in the Monte Rosa nappe. Western Alps. *Tectonics* **6**, 69–88.

Lacassin, R. (1989) Plate-scale kinematics and compatibility of crustal shear zones in the Alps. In *Alpine Tectonics*, eds M. P. Coward, D. Dietrich and R. G. Park, pp. 339–352. Geological Society of London Special Publication **45**.

Laduron, D. (1976) L'antiforme de Vanzone. Etude pétrologique et structurale dans la Valle Anzasca (Province de Novara Italie). *Memorie Istituti Geologia e Mineralogia di Padova, Italia* **28**, 1–121.

Lagabrielle, Y., Fudral, S. and Kiénast, J.-R. (1989) La couverture océanique des ultrabasites de Lanzo (Alpes occidentales): arguments lithostratigraphiques et pétrologiques. *Geodinamica Acta* **3**(2), 43–55.

Larroque, C., Calassou, S., Malavieille, J. and Chanier, F. (1995) Experimental modelling of forearc basin development during accretionary wedge growth. *Basin Research* **7**, 255–268.

Lugeon, M. (1914) Sur l'ampleur de la Nappe de Morcles. *Comptes rendus de l'Académie des Sciences, Paris* **158**, 2029–2030.

Malavieille, J. (1984) Modélisation expérimentale des chevauchements imbriqués: appliquation aux chaînes de montagne. *Bulletin de la Société Géologique de France* **26**, 129–138.

Malavieille, J. (1995) Influence of initial geodynamic settings on the structure and evolution of collision belts, from subduction to late orogenic collapse. In *Third Sino-French Symposium on active collision in Taiwan, ACT Symposium*, pp. 251–262.

Malavieille, J., Larroque, C. and Calassou, S. (1993) Modélisation expérimentale des relations tectonique/sédimentation entre bassin avant-arc et prisme d'accrétion. *Comptes rendus de l'Académie des Sciences, Paris* **316**, 1131–1137.

Marchant, R. (1993) The underground of the Western Alps. *Mémoires de Géologie de Lausanne* **15**, 1–137.

Marchant, R. and Stampfli, G. (1997) Crustal and lithospheric structures of the Western Alps: geodynamic significance. In *Deep Structure of the Swiss Alps: Results of the National Research Program 20 (NRP 20)*, eds O. A. Pfiffner, P. Lehner, P. Heitzmann, S. Mueller and A. Steck, pp. 326–337. Birkhäuser, Basel.

Marthaler, M. and Stampfli, G. (1989) Les Schistes lustrés à ophiolites de la nappe du Tsaté: Un ancien prisme d'accretion issu de la marge active apulienne. *Schweizerische Mineralogische Petrographische Mitteilungen* **69**(2), 211 216.

Merle, O. and Ballèvre, M. (1992) Late Cretaceous–Early Tertiary detachment fault in the Western Alps. *Comptes rendus de l'Académie des Sciences, Paris* **315**(II), 1769–1776.

Meyer, J. (1983) Mineralogie und petrologie des allalingabbros. Unpublished PhD. thesis, University of Basel.

Michard, A., Chopin, C. and Henry, C. (1993) Compression versus extension in the exhumation of the Dora-Maira coesite-bearing unit Western Alps, Italy. *Tectonophysics* **221**, 173–193.

Oberhänsli, R., Hunziker, J. C., Martinotti, G. and Stern, W. B. (1985) Geochemistry, geochronology and petrology of Monte Mucrone: an example of eo-Alpine eclogitization of Permian granitoids in the Sesia-Lanzo zone Western Alpes, Italy. *Chemical Geology Isotopic Geoscience Section* **52**, 165–184.

Pfeiffer, H. R., Colombi, A. and Ganguin, J. (1989) Zermatt-Saas and Antrona zone: a geochemical comparison of polymetamorphic ophiolites of the central Alps. *Schweizerische Mineralogische Petrographische Mitteilungen* **69**, 217–236.

Pfeiffer, H. R., Colombi, A., Ganguin, J., Hunziker, J., Oberhänsli, R. and Santini, L. (1991) Relics of high-pressure metamorphism in different lithologies of the Central Alps: an updated inventory. *Schweizerische Mineralogische Petrographische Mitteilungen* **71**, 441–451.

Pfiffner, O. A. (1992) Tectonic evolution of Europe–Alpine orogeny. In *A Continent Revealed—The European Geotraverse*, eds D. Blundell, R. Freeman and S. Mueller, pp. 180–189. Cambridge University Press, Cambridge.

Pfiffner, O. A., Levato, L. and Valasek, P. (1991) Crustal reflections from the Alpine orogen: Results from deep seismic profiling. In *Continental Lithosphere: Deep Seismic Reflections* eds R. Meissner, L. Brown, H. J. Dürbaum, W. Franke, K. Fuchs and F. Seifert, pp. 185–193. American Geophysical Union, Geodynamic Series **22**.

Platt, J. P. (1986) Dynamics of orogenic wedges and the uplift of high-pressure metamorphic rocks. *Bulletin of the Geological Society of America* **97**, 1037–1053.

Pognante, U., Talarico, F. and Benna, P. (1988) Incomplete blueschist recrystallization in high-grade metamorphics from the Sesia-Lanzo unit (Vasario-Sparone subunit, Western Alps): a case history of metastability. *Lithos* **21**, 129–142.

Ramsay, J. G. and Huber, M. I. (1987) *The Techniques of Modern Structural Geology*, Vol. 2, p. 620. Academic Press, New York.

Rivalenti, G., Rossi, A., Siena, F. and Sinigoi, S. (1984) The layered series of the Ivrea-Verbano igneous complex Western Alps, Italy. *Tschermaks Mineralogische Petrographische Mitteilungen* **33**, 77–99.

Roeder, D. (1989) South-Alpine thrusting and trans-Alpine convergence. In *Alpine Tectonics*, ed. M. P. Coward, D. Dietrich and R. G. Park, pp. 47–63. Geological Society of London Special Publication **45**.

Ruppel, C., Royden, L. and Hodges, K. V. (1988) Thermal modeling of extensional tectonics: Application to temperature–pressure–time histories of metamorphic rocks. *Tectonics* **7**, 947–957.

Rutter, E. H. (1986) On the nomenclature of mode of failure transitions in rocks. *Tectonophysics* **122**, 381–387.

Rutter, E. H., Brodie, K. H. and Evans, P. J. (1993) Structural geometry, lower crustal magmatic underplating and lithospheric stretching in the Ivrea-Verbano zone, northern Italy. *Journal of Structural Geology* **15**, 647–662.

Sartori, M. (1990) L'Unité du Barrhorn (Zone Pennique, Valais, Suisse), un lien entre les Préalpes médianes rigides et leur socle paléozoique. *Mémoires de Géologie de Lausanne* **6**, 1–156.

Schardt, H. (1907) Les vues modernes sur la tectonique et l'origine de la chaîne des Alpes. *Arch. Sci. phys. nat.* **4**, 356–385, 483–496.

Schmid, R. (1967) Zur Petrographie und Structur der Zone Ivrea-Verbano zwischen Valle d'Ossola und Val Grande (Prov. Novara, Italien). *Schweizerische Mineralogische Petrographische Mitteilungen* **47**, 935–1117.

Schmid, S. M., Rück, P. and Schreurs, G. (1990) The significance of the Schams nappes for the reconstruction of the palaeotectonic and orogenic evolution of the Penninic zone along the NFP-20 East traverse (Grisons, eastern Switzerland). *Mémoires de la Société Géologique de France (n.s.)* **156**, 263–287.

Schmid, S. M. and Handy, M. R. (1991) Towards a genetic classification of fault rocks: geological usage and tectonophysical implications. In *Controversies in Modern Geology*, Vol. 16, pp. 340–360. Academic Press, New York.

Schmid, S. M., Pfiffner, O. A., Schönborn, G., Froitzheim, N. and Kissling, E. (1997) Integrated cross section and tectonic evolution of the Alps along the eastern transect. In *Deep structure of the Swiss Alps: Results of the National Research Program 20 (NRP 20)*, eds O. A. Pfiffner, P. Lehner, P. Heitzmann, S. Mueller and A. Steck, pp. 289–304. Birkhäuser, Basel.

Shreve, R. L. and Cloos, M. (1986) Dynamics of sediment subduction, melange formation and prism accretion. *Journal of Geophysical Research* **91**, 10229–10245.

Stampfli, G. (1993) Le Briançonnais, terrain exotique dans les Alpes? *Eclogae Geologicae Helvetiae* **86**, 1–45.

Stampfli, G. and Marthaler, M. (1990) Divergent and convergent margins in the North-Western Alps. Confrontation to actualistic models. *Geodinamica Acta* **4**(3), 159–184.

Stampfli, G., Marcoux, J. and Baud, A. (1991) Tethian margins in space and time. *Paleogeography, Paleoecology, Paleoclimatology* **87**, 373–409.

Steck, A. (1984) Structures de déformation tertiaires dans les Alpes centrales. *Eclogae Geologicae Helvetiae* **77**, 55–100.

Steck, A. (1987) Le massif du Simplon. Réflexions sur la cinématique des nappes de gneiss. *Schweizerische Mineralogische Petrographische Mitteilungen* **67**, 27–45.

Steck, A. (1989) Structures des déformations alpines dans la région de Zermatt. *Schweizerische Mineralogische Petrographische Mitteilungen* **69**, 205–210.

Steck, A. (1990) Une carte des zones de cisaillement ductile des Alpes Centrales. *Eclogae Geologicae Helvetiae* **83**, 603–627.

Steck, A., Epard, J.-L., Escher, A., Marchant, R. and Masson, H. (1997) Geological interpretation of the seismic profiles through Western Switzerland: Rawil (W1), Val d'Anniviers (W2), Mattertal (W3), Zmutt-Zermatt-Findelen (W4) and Val de Bagnes (W5). In *Deep structure of the Swiss Alps: Results of the National Research Program 20 (NRP 20)*, eds O. A. Pfiffner, P. Lehner, P. Heitzmann, S. Mueller and A. Steck, pp. 123–138. Birkhäuser, Basel.

Steck, A., Epard, J.-L., Escher, A., Marchand, R., Masson, H. and Spring, L. (1989) Coupe tectonique horizontale des Alpes centrales. *Mémoires de Géologie de Lausanne* **5**, 9.

Steck, A. and Hunziker, J. C. (1994) The Tertiary structural and thermal evolution of the central Alps—compressional and extensional structures in an orogenic belt. *Tectonophysics* **238**, 229–254.

Steck, A. and Tièche, J.-C. (1976) Carte géologique de l'antiforme péridotitique de Finero avec des observations sur les phases de déformation et de recristallisation. *Schweizerische Mineralogische Petrographische Mitteilungen* **56**, 501–512.

Tardy, M., Deville, E., Fudral, S., Guellec, S., Ménard, G., Thouvenot, F. and Vialon, P. (1990) Interprétation structurale des données du profil sismique réflexion profonde Ecors-Crop Alpes entre le front Pennique et la ligne du Canavese. In *Deep structure of the Alps*, eds F. Roure, P. Heitzmann and R. Polino, pp. 217–226. Mémoires de la Société Géologique de France, Paris **156**.

Trümpy, R. (1973) The timing of orogenic events in the Central Alps. In *Gravity and Tectonics*. Wiley, New York.

Trümpy, R. (1980) An outline of the geology of Switzerland. In *Geology of Switzerland, A Guide Book, Part A*, p. 104. Wepf and Co., Basel.

Trümpy, R. (1988) A possible Jurassic–Cretaceous transform system in the Alps and the Carpathians. *Geological Society of America Special Paper* **218**, 93–109.

Trümpy, R. (1992) Ostalpen und Westalpen-Verbindendes and Trennendes. *Jahrbuch Geologie B.-A.* **135**(4), 875–882.

Venturini, G. (1995) Geology, geochemistry and geochronology of the inner central Sesia Zone (Western Alps—Italy). *Mémoires de Géologie de Lausanne* **25**, 1–150.

Venturini, G., Martinotti, G. and Hunziker, J. C. (1991) The protoliths of the 'ecologitic micaschists' in the lower Aosta Valley (Sesia-Lanzo zone, western Alps). *Memorie Istituti di Geologia e Mineralogia di Padova, Italia* **43**, 347–359.

Vuichard, J. P. (1989) La marge austroalpine durant la collision alpine: évolution tectono-métamorphique de la zone Sesia-Lanzo. *Mémoire, Documentation du Centre Armoricain d'étude Structurale des Socles* **24**, 307.

Willett, S. D., Beaumont, C. and Fullsack, P. (1993) Mechanical model for the tectonics of doubly vergent compressional orogens. *Geology* **21**, 371–374.

Zingg, A., Handy, M. R., Hunziker, J. C. and Schmid, S. M. (1990) Tectonometamorphic history of the Ivrea zone and its relationship to the evolution of the Southern Alps. *Tectonophysics* **182**, 169–192.